# Estimates of Phytoplankton carbon from high-resolution optical sensors in the Southern Ocean.

By

Ogunkoya Ayodele Gilbert

Supervised by

A/Prof. Marcello Vichi

Dr Sandy Thomalla

Dissertation submitted in Partial fulfillment of the Requirement for the degree of Master of Science (Taught)

Department of Biological sciences, University of Cape Town

February 2014



UNIVERSITY OF CAPE TOWN
IYUNIVESITHI YASEKAPA • UNIVERSITEIT VAN KAAPSTAD

UNIVERSITY OF CAPE TOWN
Marine Research Institute

Plagiarism declaration

I know the meaning of plagiarism and declare that all the work in this dissertation, save for that which is properly acknowledged, is my own.

……

Ogunkoya Ayodele Gilbert

## Abstract

Phytoplankton is an important component of the oceanic carbon cycle, and deriving a good estimate of its carbon biomass ($C_{phyto}$) at ocean scale is difficult due to the lack of automatic sampling procedures. This is particularly difficult in the Southern Ocean, where winter conditions limit the sampling. This study explored the opportunity of using a high resolution data from the glider tracks in the Sub-Antarctic Zone of the Southern Ocean. The data consisted of particulate backscattering and chlorophyll and four different methods of estimating phytoplankton carbon were used, three of them based on backscattering (named 30%POC, B05 and M13) and one on chlorophyll (S09). The methods are different in their empirical formulations and source of original data. Three methods showed similar results despite the fact that one of them makes use of chlorophyll to derive $C_{phyto}$. Method M13 doubles that of the 3 other methods (~ 80 mg C $m^{-3}$ vs 40-50 mg C $m^{-3}$). It was observed that discrepancy between M13 and the other 3 methods decreases with depth and when biomass was low (~0.25 mg Chl-*a* $m^{-3}$) e.g., at depth 80 m. Investigating the drivers of variability in chl-*a*:$C_{phyto}$ ratios with depth and MLD shows little response and highlighted the need for more research in this region. Although M13 has a very low chl-*a*:$C_{phyto}$ ratios, the range of variability was similar to that of the 30%POC and B05 methods and likely driven by variability in light and Fe limitation and changes in community structure. Despite a similar magnitude, the S09 method show a tight constrain in chl-*a*:$C_{phyto}$ ratios that were methodologically driven and thus less sensitive to physiological adjustments in cellular chl-*a*:$C_{phyto}$ ratios. The analysis also

confirms that each oceanic region has factors that drive their variability and care needs to be taken when applying a method that was derived from one oceanic region to another.

## Dedication

This project is dedicated to God the Father, Son and the Holy Spirit. For great things he has done in my life and to my Late mother Adebimpe Silifatu Ogunkoya (nee QUADRI).

I love you sweet mother but God loves you most. Continue to rest in peace till the day we meet and part no more.

**Acknowledgements**

I want to say a big thank you to my two supervisors: Marcello Vichi, from Oceanography Department for his constructive criticism and feedback and Sandy Thomalla, from the CSIR for her endless patience, encouragement and invaluable feedback and for the data used for this research.

I am forever grateful to my family, my father Babatunde for his financial and moral support. My sister and brothers, Omolola, Damilola and Sasaeniya Ogunkoya. I love you so much and pray that God will continue to bless you. My beautiful and sweet daughter Oluwanifemi Aviela, I love you so much, your birth has really pushed me to want to achieve more in life so that I can give you the best of life. I want to say a big thank you to my confidant, my one and only Gudrun Pontes. You are God sent, thanks for the moral and financial support.

A big thank you to my friends Sege benson, Oscar-Deno, Jude, Tega, Best Gaaji, Olumide and Walesdonal, thank you all for your support and care. To my fellow Ma-Re 2014 colleagues, thank you for all the love and care during the time we were together. A big hug to staff of Ma-re, Pavs Pillay, Charine, Sharon Bosman, Gilly Smith, Soraya Abraham, Bolarin and the Secretary at the Department of Biological Sciences you made my study year stress-free.

This project would have not been possible if not for the financial grant from the Marine Research Institute (Ma-Re).

# TABLE OF CONTENTS

# 1. GENERAL INTRODUCTION

## 1.1 The role of phytoplankton in the global carbon cycle and climate

The ocean has a primary role on climate regulations through the exchange of freshwater, heat and carbon with the atmosphere. The ocean has absorbed nearly 93% of the surplus heat energy derived from anthropogenic radiative perturbation over the last fifty years (Church *et al.,* 2011; Levitus *et al.,* 2012). The capability of the ocean to store large quantity of heat is mostly due to the large mass and heat capacity of seawater relative to air and the circulation of the ocean connects the surface and ocean interior. This is because more than ¾ of the total exchange of water between the Earth's surface and atmosphere through precipitation and evaporation takes place over the oceans (Schmitt, 2008). Albeysirigunawardena and Walker, (2008) said that "it is virtually certain that the upper ocean (above 700 m) has warmed from 1971, and it is likely that it has warmed from 1870s to 1971". This is based on the data collected since 1971 from independent observation of the subsurface temperature, seas surface temperature and sea level rise (Rhein *et al.,* 2013).

The world's ocean is also the largest deposit of $CO_2$ in the Earth system (Yool *et al.,* 2007). The oceans help the world's climate by their unique capacity to absorb $CO_2$, which slows down the effects of carbon emission derived from human activities (Bindoff *et al.,* 2007; Figure 1.1). The oceans absorbed 2.9 ± 0.5 Pg C $y^{-1}$ in 2013, which was slightly above the average of 2.6 ± 0.5 Pg C $y^{-1}$ over the period 2004 - 2013. Fossil fuel and cement account for a total cumulative emission of 390 ± 20 Pg C from 1870 to 2013, while the total cumulative from change in land use during the same period accounts for 145±50 Pg C.

During this same period the ocean has absorbed 150 ± 20 Pg C (Global Carbon Project, 2014).

Part of this service of absorbing anthropogenic carbon is operated by the marine primary producers. Marine phytoplankton has an average biomass turnover that ranges between 1 to 2 weeks and still, these temporary living organisms can absorb carbon at a rate of 40-50 Pg C $y^{-1}$ and are responsible for roughly half the primary production of the world (Antoine *et al.,* 1996; Field *et al.,* 1998; Falkowski *et al.,* 1998, Westberry *et al.,* 2008). Roughly 10 Pg C $y^{-1}$ of this production is deposited at a depth of 100 m and below and are exported by sinking particles (Bishop, 2009). This fast and rapid process is termed the "biological carbon pump" (Figure 1.2; Volk and Hoffert, 1985; Broecker and Peng 1992). It is essential to the future control of atmospheric $CO_2$ (Siegenthaler and Sarmiento, 1993) and also very important because it determines the vertical distribution of carbon in the world ocean and thus the $CO_2$ surface pressure, which controls the sea-air exchange (Bishop, 2009).

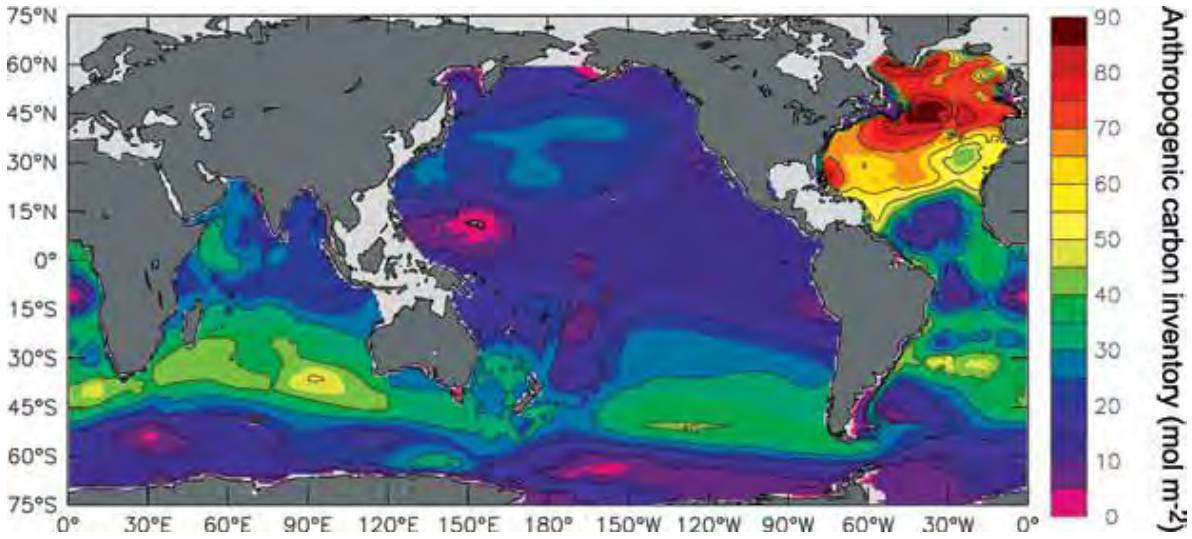


**Figure 1.1.** The global ocean uptake of anthropogenic carbon from 1750 to 1985. The Northern Atlantic (top right corner) is responsible for the largest absorption of anthropogenic carbon since pre-industrial times and the mid-latitude Southern Ocean (about 30°S and 50°S) Figure reproduced from Bindoff *et al.*, (2007). (ACE CRC, 2011).

In the Southern Hemisphere, large part of the regulation of long-term climate is undertaken by the Southern Ocean. The ability of the Southern Ocean to store heat helps in controlling the warming of the Southern Hemisphere. Southern Ocean is responsible for 40% of global $CO_2$ uptake (Gruber *et al.,* 2009), its warming will cause ocean stratification, which would lead to a decrease in $CO_2$ uptake and subsequently lead to increase in Southern Hemisphere ocean temperature (ACE CRC, 2011). The Sub Antarctic Zone (SAZ) is located further south of sub-tropical waters of the Southern Hemisphere. The SAZ is a strong sink for $CO_2$ as reported by Metzl *et al.,* 1999, 2006; McNeil *et al.,* 2007; Takahashi *et al.,* 2012; Lenton *et al.,* 2013. This is because biological production increases in summer and tends to reduce the $pCO_2$ thereby increasing the net uptake of $CO_2$. In winter, when biological production is low, the SAZ is able to sink $CO_2$ as a result of deep winter mixing entraining carbon rich waters from the ocean interior into the surface mixed layer.

Despite this central role in the Earth system, the Southern Ocean is one of the most under studied oceans in the world and there is inadequate knowledge about how it is expected to respond to climate change (Monteiro *et al.,* 2010, Lenton *et al.,* 2013). This is due largely to logistical difficulties in data collection over appropriate temporal and spatial scales (Hiscock *et al.,* 2007). While satellite remote sensing provides broad scale surface data for investigating patterns of phytoplankton variability, they only measure proxies of phytoplankton biomass and not the actual carbon. Chlorophyll is a legitimate measure of phytoplankton biomass for some application, for example, certain models of primary production that use chlorophyll, and not carbon as the state variable. There are many other legitimate measures of phytoplankton biomass, including carbon and nitrogen content. Clearly, for work that requires carbon biomass, chlorophyll biomass from satellites is not adequate. That is why efforts to estimate phytoplankton carbon are so valuable. Regular *in situ* observations over depth from autonomous instrument (e.g., gliders, and bio-optics floats) are essential to increase the capability of capturing higher frequency changes of the ocean biogeochemistry (Boss *et al.,* 2008). It is therefore important for us to put effort into developing the best methods of detecting biogeochemical parameters from instruments on autonomous platforms. In particular, given the importance of phytoplankton production in driving the carbon sink, it is important to get good estimates of phytoplankton carbon (Boss *et al.,* 2008).

Bio-optics is one of the disciplines of science that studies the properties of the ocean through their interaction with the light. It is the principle at the basis of satellite ocean color measurements, which rely on the light absorption by phytoplankton chlorophyll (prevalently chlorophyll-a concentration). However, particles in the ocean also have light

scattering properties (e.g., backscattering and beam attenuation) that have been proposed as a possible index of estimating phytoplankton biomass in addition to chlorophyll-a concentration. The advantage is that, it is believed to be less responsive to environmental conditions affecting the physiology of organisms (e.g., nutrients and light) that changes the intracellular pigment concentrations. The only problem of particulate backscattering is that it is not unique to phytoplankton (Dall'Olmo *et al.,* 2009).

This project contribute to research carried out by the Southern Ocean Carbon and Climate Observatory (SOCCO; www.socco.org.za) and is based on data collected in the Sub-Antarctic Zone of the Southern Ocean during the Southern Ocean Seasonal Cycle Experiment (SOSCEx) from austral winter 2012 to late summer 2013 using high resolution glider. In this study the aim is to understand the implication of using backscattering and chlorophyll methods of deriving phytoplankton carbon ($C_{phyto}$) and to understand if a method of deriving phytoplankton carbon using data from different oceanic region can be applied to all oceans. As previous studies has shown the importance of phytoplankton in the ocean, a good estimate will enable us to understand more better the role they play in biological pump in regulating Earth climate.

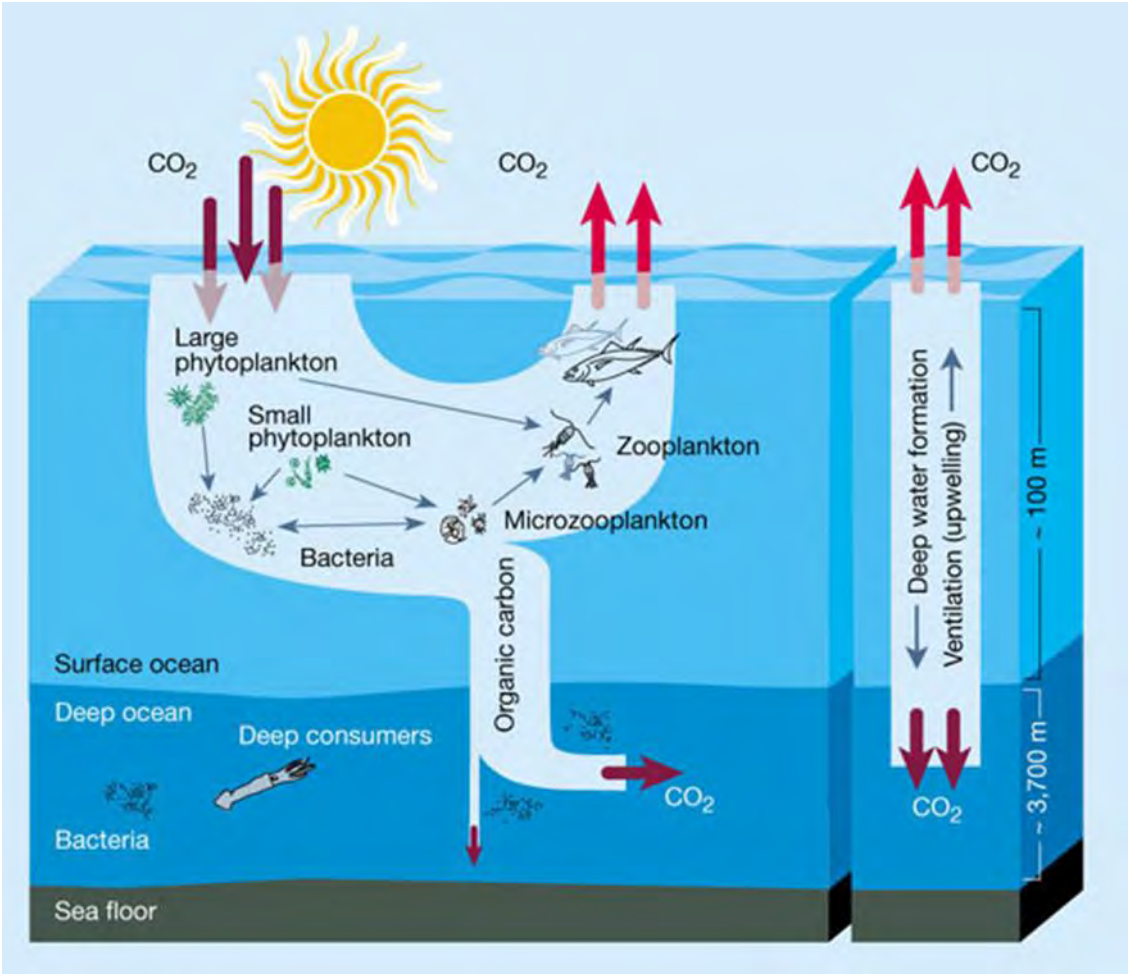


**Figure 1.2** Biological pump and the "solubility pump" (right), this is driven by physical and chemical processes. Figure reproduced from Oceanography: Stirring times in the Southern Ocean Sallie W. Chisholm Nature 407, 685-687(12 October 2000) doi: 10.1038/35037696.

# 2 Literature Review

## 2.1 The Southern Ocean

The Southern Ocean consists of the southern portion of the Pacific, Atlantic and Indian oceans. It unique circumpolar geometry of an open channel and merging waters from other regions such as the Pacific, Atlantic and Indian Oceans (Watson *et al.,* 2014). The Southern Ocean is unbroken by any other continental landmass and its narrowest constriction is the Drake Passage, 600 miles wide (about 1000 km), between South America and the tip of the Antarctic Peninsula (Encyclopedia Britannica, 2014). The Southern Ocean is fundamental to the earth climate, but still find it difficult to comprehend its uniqueness (Watson *et al.,* 2014). The role of the Southern Ocean is substantial, from carbon fixing to the physical and biological pumps, as well as thermohaline circulation (e.g. Antarctic Intermediate Water formation and sub-Antarctic Mode Water, see Tally *et al.,* 2008). It also plays a very important role supplying nutrients to the thermocline water of the whole Southern Hemisphere as well as the North Atlantic. (Sarmiento *et al.,* 2004b). The Southern Ocean is one of the most important sources of short-term unpredictability in terms of $CO_2$ fluxes particularly at the seasonal scale (Lenton *et al.,* 2013). It is the only region of the Earth where deep-ocean $CO_2$ repository (~38 000 Gt C) exchange directly with the smaller atmospheric repository (~700 Gt C; Swart *et al.,* 2012).

The Antarctic Circumpolar Current (ACC) is the major current of the Southern Ocean and the largest current in the world, it links the basins of the Indian, Atlantic and Pacific oceans (Fig.2.1; Rintoul, 2011).

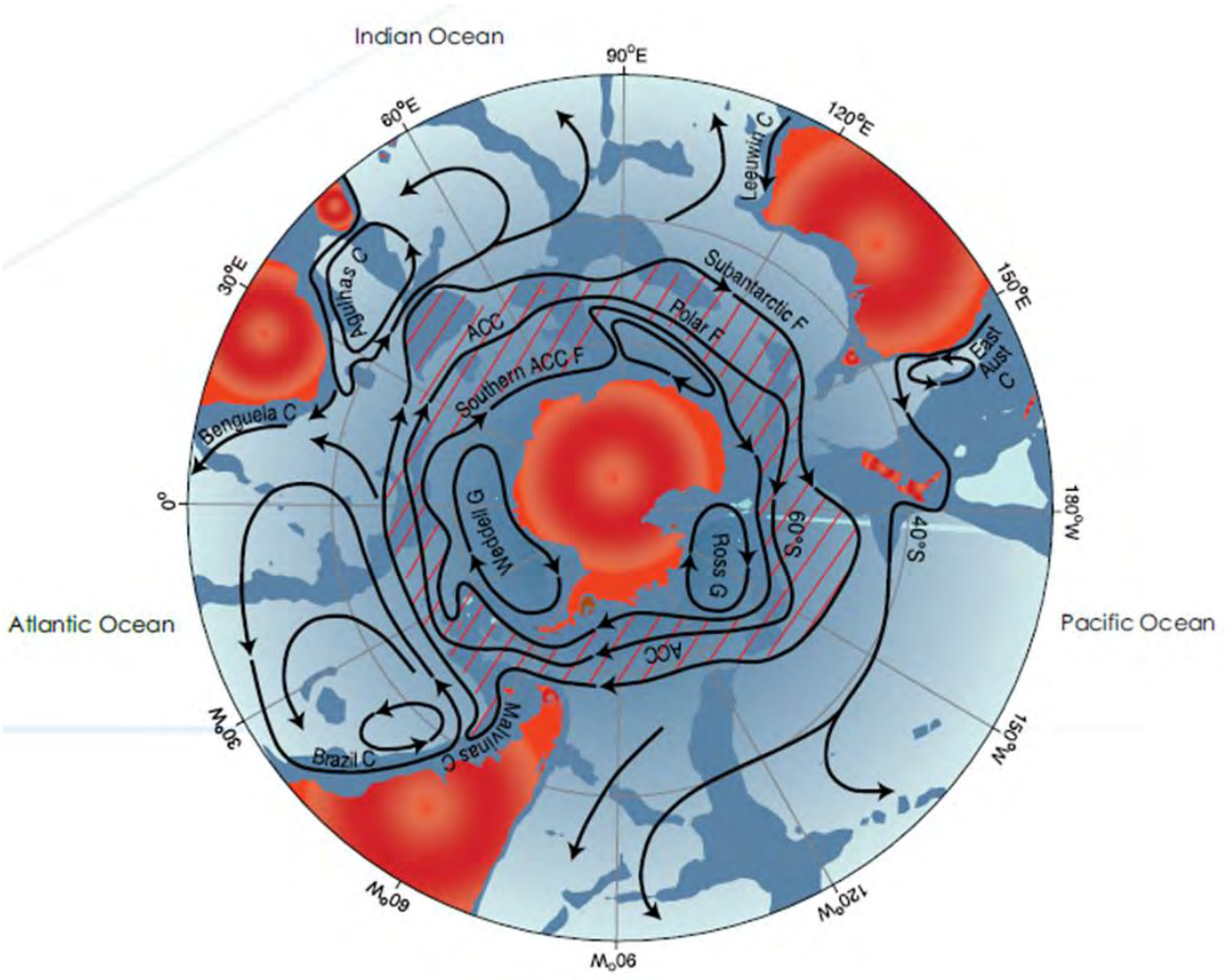


Figure 2.1 Diagram of the Southern ocean showing the mean surface flow features: the hatched area shows the broad scale flow in the ACC. Dark(light) blue region show ocean depth less than 2000 m. ACC = Antarctic Circumpolar Current): F=Front; G = Gyre. Figure reproduced from Rintoul (2011).

The circumpolar fronts divide the Southern Ocean into 3 three distinct oceanographic zones. They are the Subantarctic Zone (SAZ), Polar Frontal Zone, Southern Front (Antarctic Zone and Continental Zone; Orsi *et al.,* 1995). The SAZ extends south from the Subtropical Front (STF), the boundary of the Southern Ocean with the Subtropical gyres, to the deep reaching Subantarctic Front (SAF), which carries the most intense transport of the Antarctic

Circumpolar Current. To the South of SAZ lies the Polar Frontal Zone, a subsurface temperature minimum that marks the northernmost extent of the Antarctic water (Trull *et al.,* 2001). The SAZ and the PFZ make up the subantarctic region (Orsi *et al.,* 1995). There are relatively large accumulations of algae in the PFZ in summer and remain constant throughout the year in the SAZ, both region has high chlorophyll concentrations than ice free circumpolar waters in the Antarctic Zone (Moore *et al.,* 2000). The phytoplankton produced fuels organic carbon export to the deep sea that is approximately close to or above the global median in both the SAZ and PFZ (Honjo *et al.,* 2000; Trull *et al.,* 2001). There is high concentration of sperm whales, which feed on cephalopods near the Southern front because of the shoaled, nutrient-rich Upper Circumpolar Deep Water. The congregation of krill, primary production, and whales with the Southern Boundary, suggests that it provides predictably productive foraging for many species, making it important to the function of the Southern Ocean ecosystem (Tynan, 1998).

The extreme and unique properties of the environment of the Southern Ocean makes it an important place to harbor and shelter unique ecosystems. The Southern Ocean has a low phytoplankton biomass in spite of the high concentration of macronutrients, this is due to limited micronutrients (iron; Rintoul *et al.,* 2009). However it is difficult to estimate and explain long term trends of the ecological and biological time series because they are insufficient, short and restricted to a particular area. Usually, the chemical and environmental quantification required to join the environmental and ecosystem variability together are absent (Rintoul *et al.,* 2009). Whether these changes may impact the Southern Ocean carbon cycle is even more uncertain.

## 2.2 Phytoplankton biomass in the Southern Ocean

Oceanic phytoplankton is responsible for roughly half of the global biosphere net primary production (Behrenfeld *et al.,* 2001; Field *et al.,* 1998). The metabolic demand of the marine ecosystem is fueled by the conversion of $CO_2$ into organic matter by phytoplankton. The production of phytoplankton biomass depends on the presence of sunlight and nutrients (e.g., iron, phosphorous, nitrogen) and thus prone to any changes in the physical processes controlling these resources (Boyce *et al.,* 2010). There is always a fluctuation in phytoplankton biomass relative to annual climate cycle in the ocean (Richardson *et al.,* 2010). These seasonal annual cycles are connected with annual fluctuations of the mixing, precipitation, temperature and light (Smetacek 1985; Sommer *et al.,* 1986; Cloern, 1996). These environmental factors (e.g. temperature, light etc.) can be modified by changing climatic conditions which will alter phytoplankton biomass indirectly or directly by altering the resources availability and trophic interactions (Winder and Cloern, 2010). Any future changes in the ocean primary production can potentially have a severe impact on the global carbon cycle (Gregg *et al.,* 2003).

The Southern Ocean is one of the regions of the world with high nutrient and low chlorophyll (HNLC, chl < 0.5 mg $m^{-3}$; Comiso *et al.,* 1993; Moore and Abbot, 2000). The study of the Southern Ocean has shown that the marine ecosystem has a high autotrophic biomass and primary productivity which is made up of short food chain composed of diatoms ↠ krill ↠ higher consumers (Smith and Sakshaug, 1990; Marchant and Murray, 1994).

The autotrophic biomass of the Southern Ocean is low and the base of the food chain comprises of microbial network of bacteria, phytoplankton and zooplankton (Von Brockel, 1981; Merchant and Murphy, 1994). A shift in the structure of the phytoplankton community will have a dire effect on the phytoplankton community. This is because phytoplankton are the autotrophic component of the marine ecosystem, therefore any variability would affect the efficiency and structure of the food web (Garibotti *et al.,* 2003).

The different structure of the phytoplankton community has a vital impact on the entire ecosystem because phytoplankton are the autotrophic component of the marine ecosystems and any change would definitely affects the efficiency of the food web and ability of the phytoplankton to take up $CO_2$ (Garibotti *et al.,*2003). Apart from the role of absorbing $CO_2$ from the atmosphere, phytoplankton bloom (Smayda, 1997) are indicator of annual growth activity in pelagic system of the ocean (Winder and Cloern, 2010) and obtaining a good carbon estimates of this fast growing organisms is essential. It is also essential to note that chlorophyll is a measure of phytoplankton biomass which is a proxy for primary production (Field *et al.,* 1998). This suggest of a good relationship between chlorophyll and phytoplankton biomass and effort must be put in place to further understand this two parameters to be able to fully understand the role phytoplankton plays in oceanic carbon sequestration.

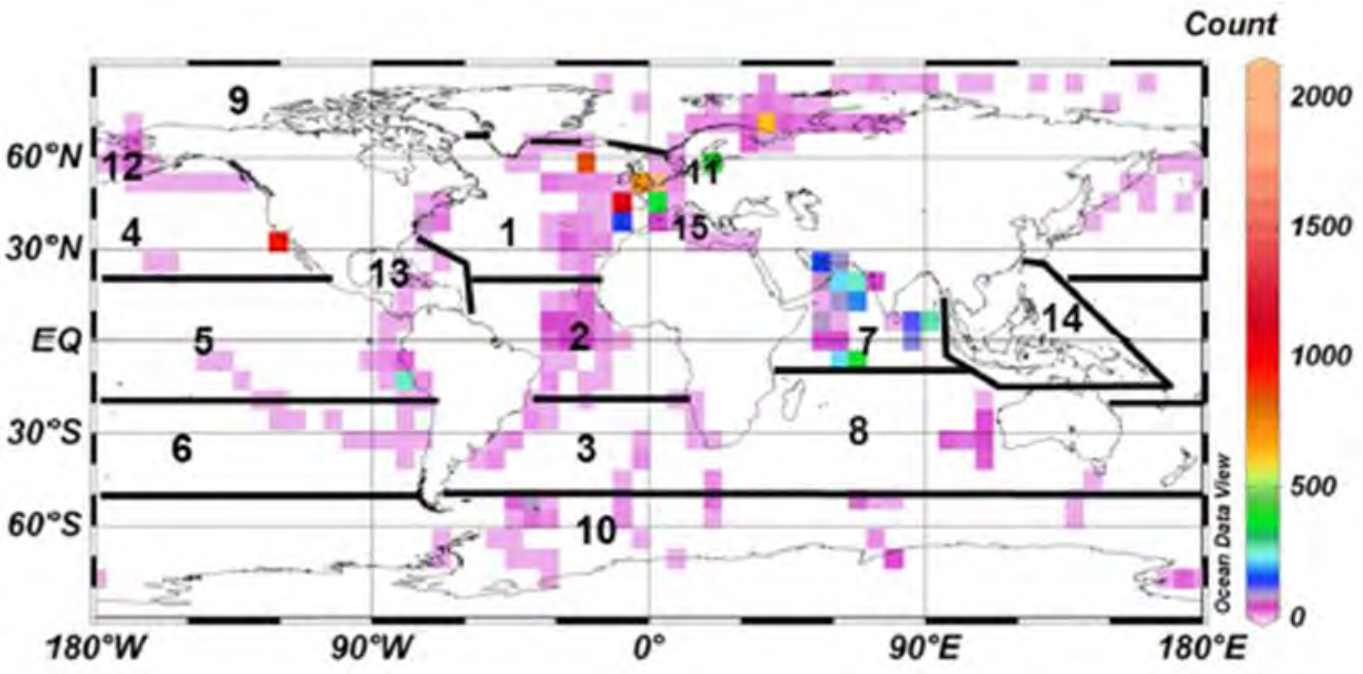


**Figure 2.2**. The Distribution of diatoms data base of the main oceanic region (1) North Atlantic, (2) Equatorial Atlantic, (3) South Atlantic, (4) North Pacific, (5) Equatorial Pacific, (6) South Pacific,(7)North Indian, (8) South Indian, (9) Arctic, (10) Antarctic, (11) Baltic Sea, (12) Bering Sea, (13) Gulf of mexico and Caribbean Sea, (14) Indonesia, and (15) Mediterranean Sea. Figure reproduce from Leblanc *et al.,* (2012).

## 2.3. Inherent Optical Properties

The Inherent optical properties (IOPs) are one of the most important tools to study many oceanic biogeochemical and ecophysiological processes at high temporal resolution sub-meter spatial scales (sub-seasonal to seasonal). E.g. IOPs data are used to derive cell sizes of phytoplankton (Ciotti *et al.,* 2002) and to estimate the growth rate of particulate organic matter (Siegel *et al.,* 2005; Claustre *et al.,* 1999). Inherent optical properties are those properties of a medium that depend on its composition (dissolved, suspended and particulate) but are independent of the incoming light, and cause changes to light intensity, spectral composition and angular distribution (Preisendorfer, 1961).

Light can undergo two pathways when entering the water; it can be absorbed (a) or scattered (b) which result in the light been attenuated (c; Fig. 2.2). Absorption result in the loss of a photon, whereas scattering causes its re-direction. Beam attenuation is thus described as the sum of the rate of radiation loss from absorption and scattering (c= a+b; Twardowski *et al.,* 2001).

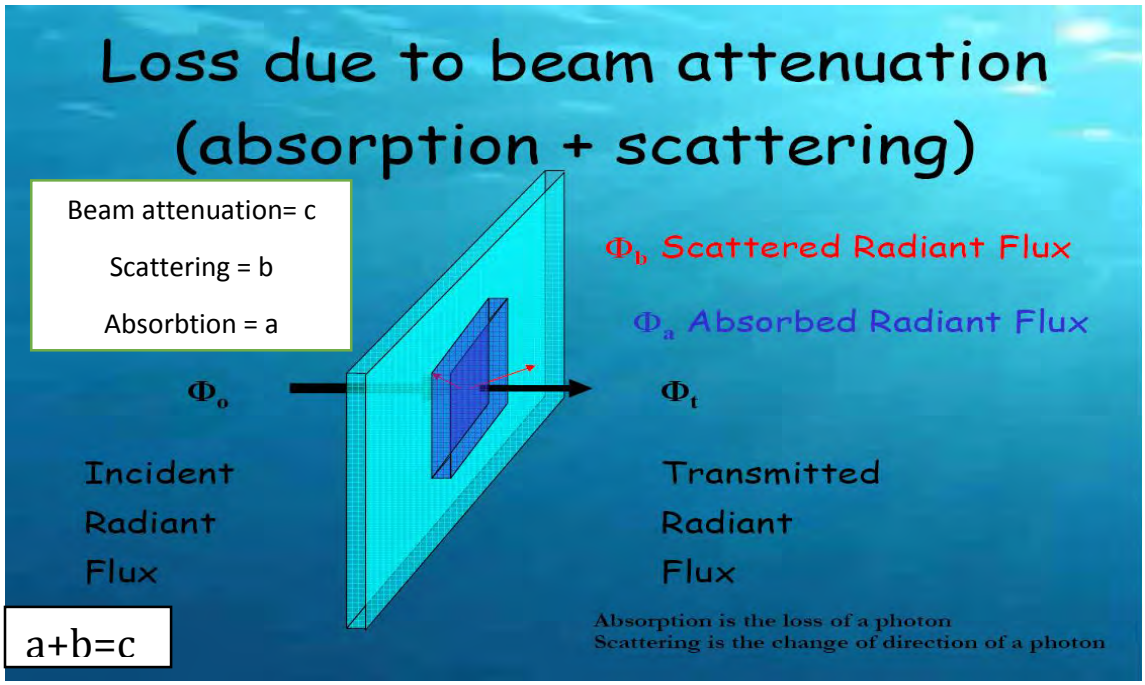


Figure 2.2 Schematic diagram of light pathway in water. Reproduced from Steward Bernard presentation.

Backscattering is approximately equal to half of scattering and makes a significant contribution to the upwelling irradiance that is observed by ocean color sensors (Falkowski and Woodhead, 1992). Particulate backscattering ($b_{bp}$) is however more affected by particles outside phytoplankton size range than it happens for particulate beam attenuation ($C_p$; Morel and Ahn,1991; Stramski and Keifer,1991). A relationship between phytoplankton carbon and $b_{bp}$ is however expected as long as the amplitude of non-algal particules contributing to the $b_{bp}$ covaries with phytoplankton biomass (Behrenfeld, 2005). Backscattering by pure water is strongest in the blue wavelengths, while particles backscatter is stronger in the red (Morel, 1974). An increase in particle concentrations is thus associated with higher backscattering in the red wavelengths. The spectral shape of backscattering also depends on the particle size, shape and composition (organic vs

minerals). For example, spectral $b_{bp}$ may also provide a proxy for particle size, which has been shown feasible using remote sensing reflectance data (Loisel *et al.,* 2006; Kostadinov *et al.,* 2009) and spectral $b_{bp}$ from glider data (Niewiadomska *et al.,*2008).

## 2.4. Phytoplankton carbon

The derivation of a good field estimate of phytoplankton carbon ($C_{phyto}$) is very important and crucial to determine the involvement of total particulate organic carbon (POC) to primary production (Winkel *et al.,* 1987; Chang *et al.,* 2003). In the ocean phytoplankton biomass is the primary food source for zooplankton (Lu *et al.,* 2009), phytoplankton biomass are usually considered as carbon content when we want to ascertain and evaluate the prey/predator relationship quantitatively and the movement of carbon through the oceanic food chain (Atkinson, 1996; Legendre *et al.,* 1999). The overlapping nature in the magnitude of phytoplankton carbon with other suspended particulate matter e.g. non-living organic matter and zooplankton makes it a very difficult task to distinguished phytoplankton carbon from other suspended particulate matter by filtration techniques when doing field measurements (Lü *et al.,*2009).

Methodological constraints result in the carbon biomass of phytoplankton to be poorly identified (Martinez –Vicente *et al.,* 2013) and distinguished from other types of carbon (Eppley *et al.,* 1992; Oubelkheir *et al.,* 2005). The ability to better quantify phytoplankton carbon would enable us to evaluate the distribution of phytoplankton biomass and understand the variability and in its response to physical drivers. In addition, accurate information on phytoplankton carbon will improve phytoplankton growth models and

better evaluate the role of phytoplankton in the global carbon cycle and how it might vary in the context of changing climate (Sathyendranath *et al.,* 2009).

The ability to differentiate phytoplankton carbon from other suspended particulate matter is still a big challenge for marine biologists. One of the method to quantify phytoplankton carbon *in situ* involves the use of bio-volume conversion rates to derive carbon biomass by empirical relationships and cell count (Strathmann, 1967). Larger phytoplankton cells can be estimated by the use of microscopy (i.e., diameter > 20µm; Holligan *et al.,* 1984), whereas smaller cells can be estimated by the use of cytometry (e.g. eukaryotes, Prochlorochoccus *spp*., Synecoccocus *spp* ; Zubkov *et al.,* 1998; DuRand *et al.,* 2001; Tarran *et al.,* 2001; Tarran *et al.,* 2006). X-ray microanalysis and Transmission electron microscopy have also been used to analyze phytoplankton biomass (Heldal *et al.,* 2003). These methods all have their own uncertainties and there is no direct, accurate and routinely performed method for measuring phytoplankton carbon at sea (Sathyendranath *et al.,* 2009). In addition, the current methods are difficult, time consuming and require researchers to be in the field or on ships (Wang *et al.,* 2012). It is thus important that methods be developed that can get phytoplankton carbon from satellites and optical sensors which are able to measure when the ships are not at sea.

Chlorophyll for a long time has been used in the field to determine phytoplankton biomass, but chlorophyll is not stable and is greatly influenced or even dominated by shifts in physiology of the intracellular pigmentation in response to changes in growth conditions (e.g. temperature, nutrients, light). Backscattering or attenuation coefficients provide a different option for optical evaluation of phytoplankton biomass that is easily assessed *in*

*situ* and comparatively insensitive to changes in content of intracellular pigment (Behrenfeld and Boss 2006), Since $b_{bp}$ is linearly related to particle content what is most easily measured by scattering sensors is total particulate carbon or total POC, of which phytoplankton carbon is recognized to be a variable fraction (Eppley *at al.,* 1992, Oubelkheir *et al.,* 2005) but it can be influenced by phenomena such as coccolithophore bloom or bubbles which can increase backscattering or the attenuation coefficient without increasing phytoplankton biomass (Sathyendranath *et al.,* 2009).

## 3 Research Aims and Objectives

See section 2.4 for review of the objectives.

The research aims of this study are to:

- Improve the Southern Ocean particulate backscattering ($b_{bp}$) and particulate organic carbon using *in situ* data.
- Apply the available methods of deriving phytoplankton carbon from high frequency optical sensors data from a glider transect in the Sub Antarctic Zone (SAZ) covering the spring/summer period.
- Analyze the effects on the carbon to chlorophyll ratio and the implication for phytoplankton as a function of time and depth.

# 4 Data and Methods

Oceanic phytoplankton are responsible for approximately 50% of the world primary production. They form the base of nearly all marine ecosystems, are important in trophic energy transfer and plays a very unique role in regulation of climate, oxygen production and carbon sequestration (Boyce *et al.,* 2010). This unique abilities of this minute organism has necessitate the need for better quantification of their carbon. The high resolution glider data used for this research, provide for the first time the application of different methods of estimating phytoplankton carbon on data from the SAZ of the Southern Ocean.

## 4.1. A Bio-optics approach: Using autonomous platforms (e.g. gliders and floats)

The Southern Ocean is a very large ocean and part of the effort to address the compexity and challenges of the Southern ocean is to invest in unmanned platforms such as Argo floats, satellites, autonomous vechicles, instruments that record information automatically (ACE CRC, 2011). The properties of the ocean can be analysed at very high frequencies by the use of autonomous platforms. Among the various autonomous platform are gliders (Figure 4.1) capable of diving at depth more than 1000m with various sensors attached to it. With gliders the ocean can be sampled at the appropriate time (sub-seasonal to seasonal) and space (meso to submesosclaes) scales that are important in linking physical forcing mechanisms with biogeochemical response like primary production and carbon export (Niewiadomska *et al.,* 2008).

Ocean colour satellite sensors provide data on surface chlorophyll concentration which is used as an indicator of phytoplankton biomass and is essential to primary productivity. However, the prevailing ocean colour algorithms applied to Southern Ocean data perform poorly, mostly due to their parametrisation with low-latitude bio-optical data sets whose characteristics are different from the Southern Ocean which underestimate chlorophyll at high-latitude (Johnson *et al.,* 2013).

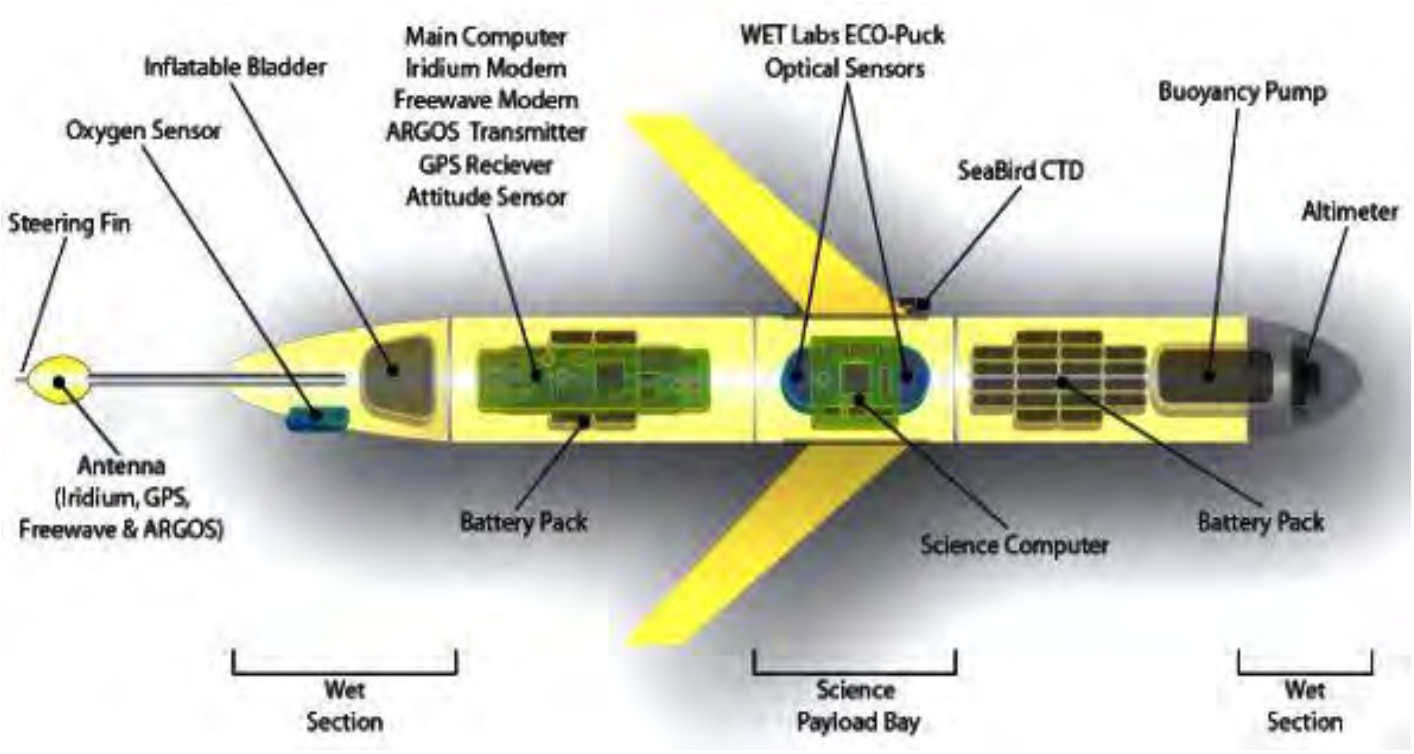


**Figure 4.1**. Schematic diagram of a glider. Image reproduced from www.solarnavigator.net.

## 4.2 The glider section

The data used for this research were collected during the Southern Ocean Seasonal Cycle Experiment (SOSCEx) which was done around five cruises to the central Subantarctic Zone (SAZ) of the Atlantic Southern Ocean South West of Africa between austral winter 2012 and the late summer of 2013. During SOSCEx, Seaglider (SG573) was deployed south of Gough Island in the South-East Atlantic Ocean at 43.0°S, 11°W (Fig. 4.1). The glider was deployed on the 20 September 2012 and retrieved on15 February 2013 and resulted in continuous sampling for 143 days (or 5.5 months; Swart *et al.,* 2014).

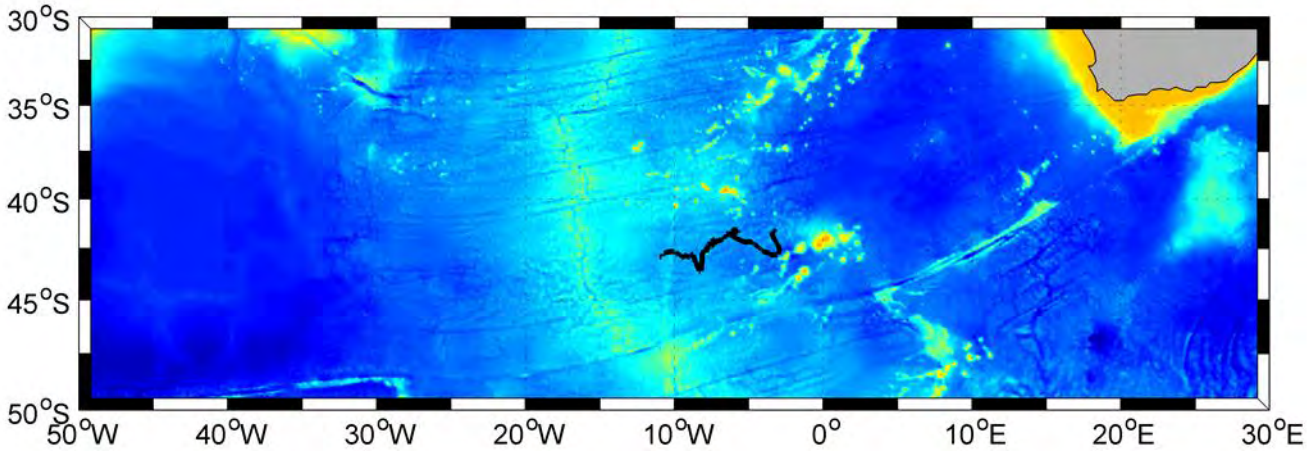


**Figure 4.2.** Trajectory of glider SG573 (black) of SOSCEx (25 September 2012–15 February 2013).

### 4.3. Glider data

The glider measured a suite of properties such as optical backscattering at two wavelengths (Bb 470 and Bb 700; a proxy for particles concentration), chlorophyll-a fluorescence; a proxy for phytoplankton concentration and other parameters such as salinity, dissolved oxygen, depth, and Photosynthetically Active Radiation (PAR; Swart *et al.,* 2014). The gliders profiled between the surface and 1000 m continuously at a nominal vertical velocity of 10 cm $s^{-1}$, with the CTD data collected at depth of 50 cm. The dive cycle took approximately 5 h to complete and covered a horizontal distance of 2.8 km on average, rendering a temporal resolution of 2.5 h and spatial resolution of 1.4 km between each water column profile (Swart *et al.,* 2014). The glider data were gridded onto a 6 hour grid to facilitate analysis. This spatial resolution covers both meso-(10–200 km) and submesoscale (1–10 km) ranges in the ocean. The glider covered a total distance of 1693 km. Data were transmitted in real-time via the Iridium satellite system upon reaching the surface after each dive. At the deployment and retrieval site of the glider, ship-based CTD cross-calibration casts were carried out yielding two independent inter-calibrations between the gliders and CTD sensors as well as bottle samples of chlorophyll-a, salinity and dissolved oxygen (Swart *et al.,*2014).

The Mixed layer depth (MLD) is defined as the depth at which the difference in temperature exceeds 0.2°C in reference to the temperature at 10 m ($\Delta T_{10m}$ = 0.2°C) was calculated following the criterion of (DeBoyer Montegut *et al.,* 2004). The Euphotic depth as the 1% light depth was calculated as the depth where PAR was 1% of the surface value.

### 4.3.1 Fluorescence derived chlorophyll-a

The instrument specific dark count was calculated as the median fluorescence value below 300 m which was then subtracted from all raw instrument counts. Florescence quenching was corrected by isolating all daylight profiles between local sunrise and sunset plus 2.5 h. The optical backscattering (Bb) was used to derive a quenching correction which is a possible indication of phytoplankton biomass in the open ocean (Behrenfeld and Boss, 2003), and is not influenced by physiological acclimation mechanisms which affect fluorescence-chlorophyll relationship in sunlit surface water. The correction was based on the methods described in Sackman *et al.,* (2008), based on the observations that at night the fluorescence to optical backscattering (FI:Bb) is relatively constant through the mixed layer. However, there is a large decrease in FI:Bb ratio in the upper layer due to day time fluorescence quenching. This method found the maximum ratio between Bb and fluorescence per profile and multiplied this ratio by Bb from the depth of the maximum to the surface to calculate a backscattering corrected fluorescence in the sunlit surface layer. On the rare occasion when backscattering was unavailable (due to intermittent sensor malfunction), fluorescence was corrected by extrapolating the maximum fluorescence value within the mixed layer to the surface.

Glider fluorescence was converted to chlorophyll using the manufacturer's instrument specific chlorophyll conversion factor and then adjusted with a statistically significant regression from 83 co-located glider chlorophyll and *in situ* chlorophyll samples (slope = 4.12, intercept = -0.21, $r^2 = 0.66$; see Swart *et al.,* 2014 for details ).

### 4.3.2. Backscattering

Spikes were separated from raw backscattering (Bb; λ=470 and 700) using a 7 point running median filter (Briggs *et al.,* 2001). Raw digital counts were converted into particulate backscattering ($b_{bp}$) according to the following equation:

$$\boldsymbol{b_{bp} = 2\pi\,\chi_p[S(Bb - D) - \beta_{sw}]} \qquad \textbf{(1 )}$$

Where $\chi_p$is equal to 1.1 and the factor used to convert to convert $\beta_p$ (at a central angle of 117°) into $\beta_{bp}$ (Boss and Pegau, 2011); *S* is the instrument specific scaling factor; *Bb* are the digital counts (λ = 470 and 700) and *D* are the dark counts; $\beta_{sw}$ is the volume scattering of pure water estimated using the models of Zhang and Hu (2009) and Zhang *et al.* (2009). Remaining spikes in particulate backscattering were removed with a threshold in shallow ($b_{bp}$> 0.048) and deep ($b_{bp}$ > 0.0025) waters. Bad profiles with high mean backscattering ($b_{bp}$ > 0.001) in deep waters (>150 m) were identified and discarded (Thomalla *et al.,* submitted).

## 4.4. Cruise Data

*In situ* data were collected on four cruises to the Southern Ocean and used to develop the methods in this thesis in combination with glider data. The cruise data makes use of high resolution CTD (6 samples per CTD in the top 150 m) with an Underway CTD (UCTD) cast between each CTD. Table 1 present the list of cruises, dates and number of samples collected. Data collected on these cruises were typically separated into three legs, the GoodHope Line between Cape Town and Antarctica (along the Greenwich meridian), the Buoy Run between Antarctica and South Georgia and the ice shelf along the continental margin (see Figure 4.3 for typical cruise tracks).

**Table 1. Dates of the various cruises indicating the different legs covered and number of samples per cruise, with leg 1 from GoodHope Line Cape Town to Antarctica, leg 2 from Antarctica to South Georgia and leg 3 to the continental ice shelf margin.**

| Cruise | Date | Leg | Number of samples |
|---|---|---|---|
| SANAE 50 | 02 Jan 2011- 01 Feb 2011 | 1,2 and 3 | 151 |
| WINTER | 09 July 2012- 01 Aug 2012 | 1 | 132 |
| SOSCEX | 18 Feb 2013-10 Mar 2013 | 1 | 89 |
| SANAE 53 | 28 Nov2013-11 Feb 2014 | 1,2 and 3 | 149 |

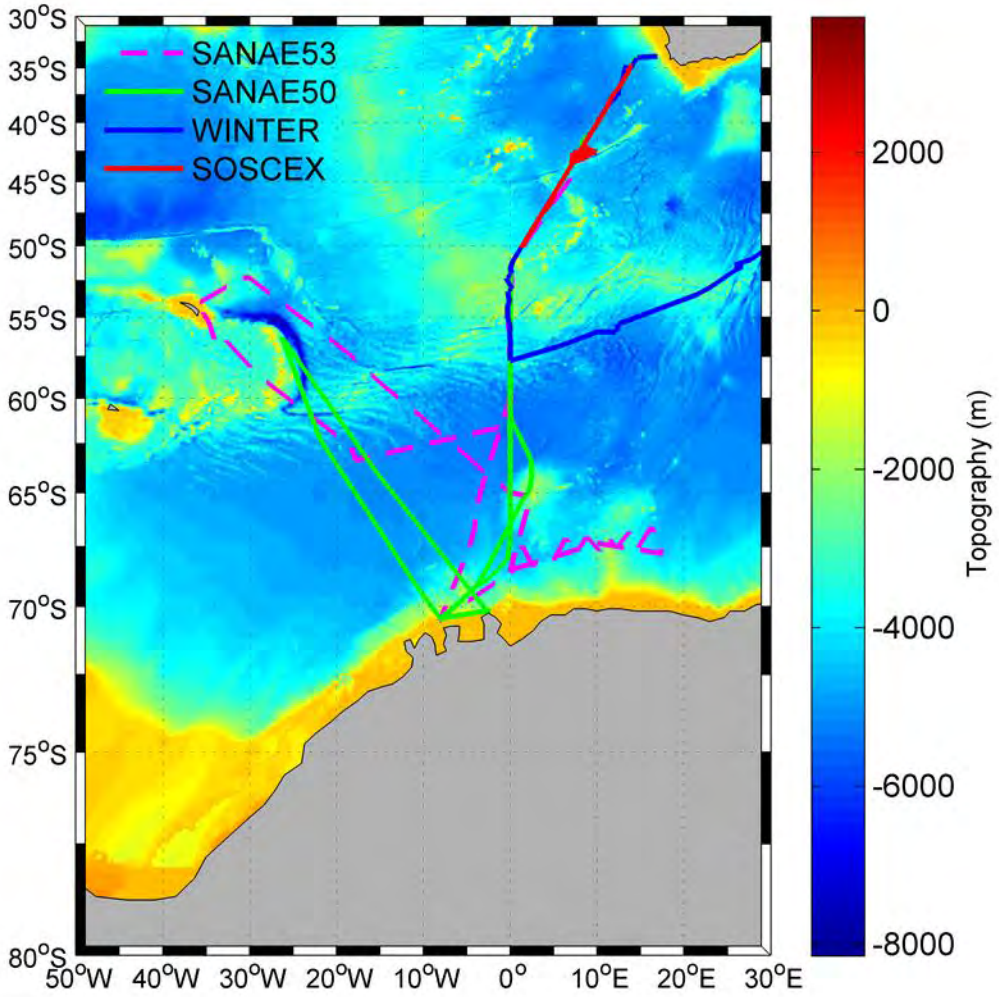


**Figure 4. 3.** Bathymetry of the study region showing all the cruise tracks. SANAE 53 in pink, SANAE 50 in green, WINTER in blue and SOSSCEx in red line.

### 4.4.1 *In situ* Chlorophyll-*a*

400 ml of sample was filtered onto Whatman 25 mm GF/F filters. The sample was later extracted in 8 ml 90% acetone and placed in the freezer for 12-24 hours. A Turner Trilogy Laboratory Fluorometer was used to measure the Chlorophyll fluorescence which was converted to concentration (mg Chl $m^{-3}$) using the calibration equation below:

$$\textbf{Chl-a} = \textbf{RF x b x } (\textbf{Vol}_e \textbf{ / vol}_s) \qquad \textbf{(2)}$$

Where RF is the measured raw fluorescence, b is the calibration factor = 0.0941 (calculated from dilution series of chlorophyll-a standard) and $vol_e$ and $vol_s$ are the volume of acetone and sample respectively. (For more details see Smith *et al.,* 2014 Master's Thesis).

### 4.4.2 Total Particulate Organic Carbon (POC)

1L Particulate Organic Carbon (POC) samples were filtered onto a pre-combusted 25 mm or 47 mm Whatmann GF/F glass fiber filters and oven dried at $50^0$C. Filters were later acidified by fuming with concentrated Hydrochloric Acid HCL for 24 hours to drive off inorganic carbon and re-dried in the oven. Filters were then pelleted into 5x8 mm tin capsules and analyzed using a CHN analyzer (Parsons *et al.,* 1984; Knap *et al.,* 1994) housed at the University of Cape Town Archaeometry Laboratory (For more details see Smith *et al.,* 2014 Master's Thesis).

## 4.5 Derivation of Phytoplankton carbon ($C_{phyto}$)

In this thesis, four different methods of deriving phytoplankton carbon ($C_{phyto}$) from backscattering and chlorophyll are applied to the glider transect in the SAZ to facilitate a comparison of the different methods. The aim of the comparison is not to criticize one methods or assume that a method is superior to other but to understand how each methods assigns carbon to phytoplankton and illuminate on the implications of using one method over another.

### 4.5.1. 30%POC method (30%POC)

Stramski *et al.,* (1999) first shows that there exist a relationship between POC and backscattering. The high correlation was a result of the dominant organic particle concentration that controls changes in both POC and $b_{bp}$ (Stramski and Morel 1990; Stramski and Reynolds, 1993; Gardner *et al.,* 1993; Marra *et al.,* 1995; Loisel and Morel, 1998).

In this method 221 POC samples from CTDs carried out on the cruises listed in Table 1 (**except** SANAE53 where no CTD POC samples were available) were plotted against co-located $b_{bp}$ 470 data extracted from CTD bottle files (i.e. the $b_{bp}$ 470 data from Niskin bottle at the time of closure). POC (Independent variable) and $b_{bp}470$ (dependent variable) were linearly correlated with one another to provide a regionally specific regression to convert $b_{bp}470$ into POC (Figure 4.3)

$$\boldsymbol{POC = 3.4*10^4 * b_{bp} + 2.8} \qquad \textbf{(3)}$$

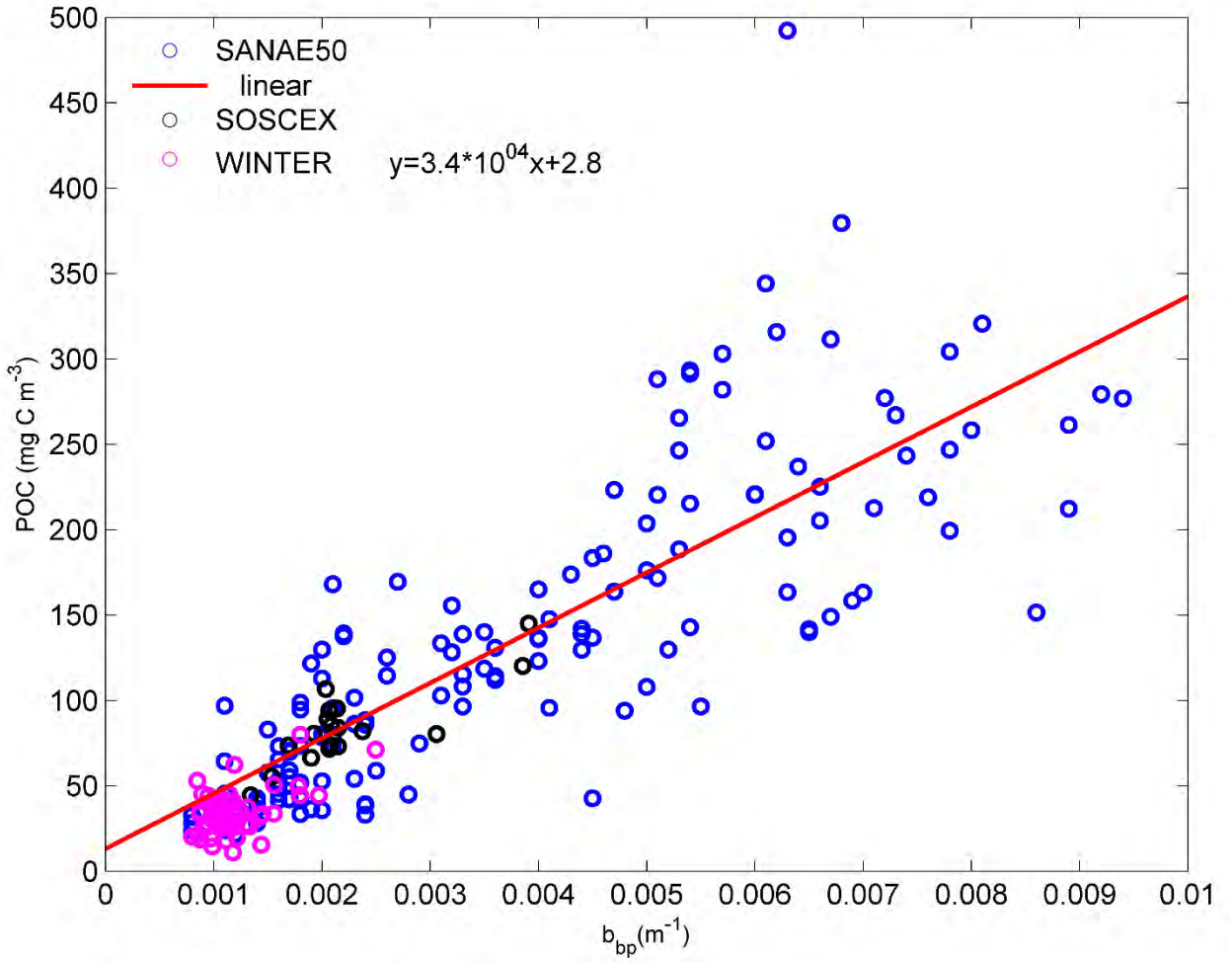


**Figure 4.4.** Relationship between POC concentration and particulate backscattering coefficient ($b_{bp}$ 470nm). R-value of 0.75

Field derived studies (Eppley *et al.,* 1992; DuRand *et al.,* 2001; Gundersen *et al.,* 2001; Oubelkheir 2001) show a range of $C_{phyto}$: POC ratios that ranges from 19% to 49% in regions from eutrophic to oligotrophic. It should be noted that some of differences that occur between previous studies are due to uncertainty in the methods used to derive phytoplankton carbon.

Behrenfeld *et al.,* (2005) summarized these ranges from estimates derived from different oceanic regions to an average phytoplankton contribution to total particulate organic carbon

range of ~ 30%. As such the 30% POC methods converts $b_{bp}$ into POC using the linear regression above (equation 3) and then converts POC to $C_{phyto}$ by reducing total POC to 30% to represent that fraction of total POC that is phytoplankton specific.

**$30\% C_{pyhto} = (3.4 * 10^{4} * b_{bp} + 2.8) * 0.3$ (4)**

### 4.5.2 Behrenfeld Method (B05)

Behrenfeld *et al.,* (2005)derived a method of estimating phytoplankton carbon biomass (mg $m^{-3}$) from remotely sensed backscattering data $b_{bp}$ using a linear relationship between $b_{bp}$ and chlorophyll (see Figure 4.5). In this method a background value of 0.00035 $m^{-1}$ is subtracted from $b_{bp}$ with the assumption that this value represent stable non-algal organisms other than phytoplankton (e.g. the detrital and heterotrophic composition of surface particle population) which also contribute to the optical backscattering signal.

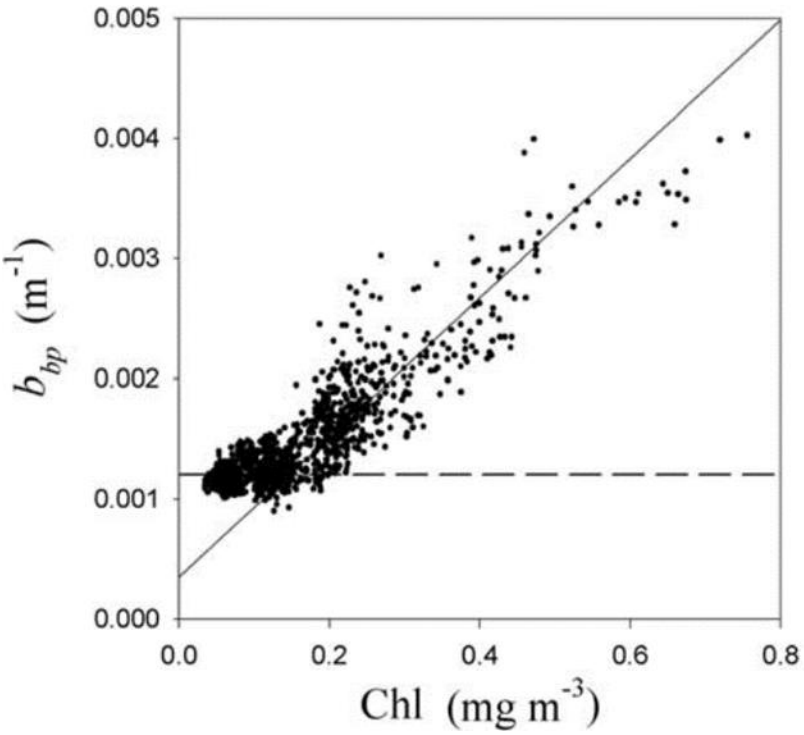


**Figure 4.5.** Regional monthly mean particulate backscattering coefficients at 440 nm (bbp) and surface chlorophyll concentrations (Chl) for the September 1997 to January 2002 period. The solid line represents a linear fit to data with Chl > 0.14 mg $m^{-3}$. The dashed line indicates the mean bbp value of 0.0012 m_1 for data where Chl < 0.14 mg $m^{-3}$ (i.e., the realm where Chl and bbp are uncorrelated). Figure reproduced from Behrenfeld *et al.,* (2005)

The corrected $b_{bp}$ is then multiplied by 13,000 mg C $m^{-2}$ to convert $b_{bp\ into}$ $C_{phyto}$. Behrenfeld *et al.,*(2005) used a scalar factor of 13 000 mg C $m^{-2}$ to give satellite Chl:C values within the range observed during laboratory experiments (average = 0.010; range = 0.002 to 0.030) as well as the average phytoplankton carbon contribution to the total particulate organic carbon of ~30% (range: 24% to 37%) which is representative of field estimates from a variety of oceanic regions of the world (Eppley *et al.,* 1992; DuRand et al., 2001; Gundersen *et al.,* 2001; Oubelkheir, 2001)

**B05 $C_{pyhto}$ = 13,000 *($b_{bp}$ - 0.00035)** **(5)**

### 4.5.3 Martinez-Vicente Method (M13).

Martinez-Vicente *et al.,* (2013) derived phytoplankton carbon from the relationship between $C_{phyto}$ and *in situ* backscattering data $b_{bp}$ (470) in the euphotic zone using in the North Atlantic using a type II linear regression (see Figure 4.6). $C_{phyto}$ concentration (in mg C $m^{-3}$) was estimated from flow cytometry for six different groups of phytoplankton according to a relationship between phytoplankton abundances (cell $m^{-3}$). Total $C_{phyto}$ concentration per sample was the addition of the contributions from each type of phytoplankton. A significant linear relationship was found between $b_{bp}$ (470) and $C_{phyto}$ when backscattering is lower than (0.003 $m^{-1}$). The author limited the linear regression to $b_{bp}$ (470) < 0.003 $m^{-1}$ because the samples above this boundary value (n=8) exhibited a shift in the relationship that was not possible to describe with a single linear function.

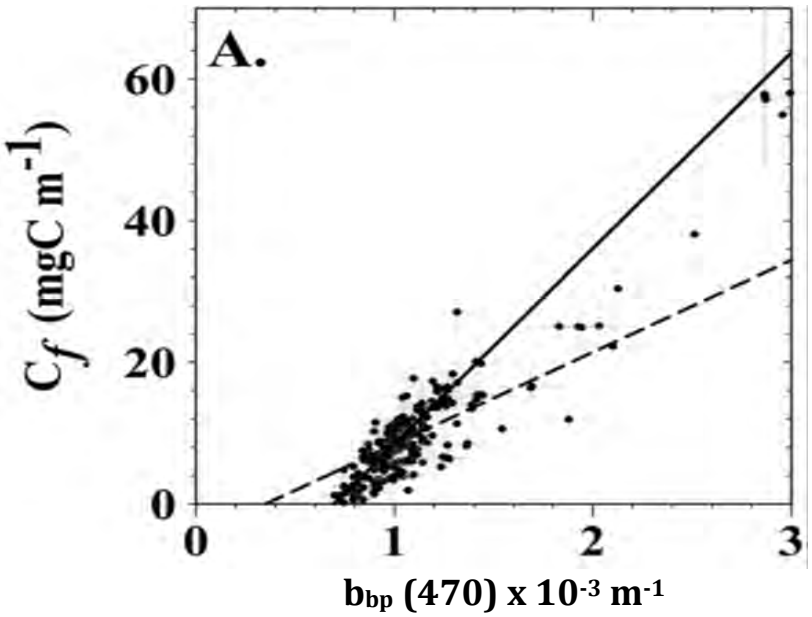


**Figure 4.6** Relationship between $b_{bp}$ (470) and phytoplankton carbon ($C_f$) (filled circles, median from Monte Carlo realizations; error bar extends from the 16th to the 84th percentiles) for $b_{bp}$ (470) <0.003$m^{-1}$. Linear regression shown by solid black line. Dash black line represents Behrenfeld et al., (2005) model for comparison. Figure taken from Martinez-Vicente *et al.,* (2013), their Figure 2a.

$$C_{phyto} = (30100 \pm 1100) * [b_{bp}(470) - (76 \pm 4) * 10^{-5}] \quad (6)$$

In this study we applied equation (6) to all glider $b_{bp}$ values, even those higher than (0.003 $m^{-1}$).

### 4.5.4 Sathyendranath's Method (S09)

Sathyendranath *et al.,* (2009) derived a method of estimating phytoplankton carbon using chlorophyll and POC observations from offshore regions of North West Atlantic (see Figure 4.7). This method assumes that at any given chlorophyll concentration, the minimum particulate carbon content observed represents the phytoplankton carbon related with that chlorophyll concentration. The authors log-transformed both POC and chlorophyll to linearize the relationship and to reduce the weight of the stations with high value of POC and chlorophyll in the regression analysis. POC as the dependent variable and chlorophyll as the independent variable are assumed to follow this non-linear model:

$$\boldsymbol{POC = a * chla^{b}}$$

which is fitted as

$$\mathbf{log}(\boldsymbol{POC}) = \boldsymbol{Log(a) + b * log(chl)}$$

where log (a) and (b) are the fitted parameters (slope and intercept respectively).

Sathyendranath *et al.,* (2009) considered that**,** since POC incorporates all types of carbon in the system which also include phytoplankton, bacteria, detritus and viruses, a more conservative estimate of $C_{phyto}$ should therefore consider only a portion of the data. They thus used a 1% quantile regression to represent the lowest particle content from phytoplankton alone (thus excluding carbon contributions from bacteria, detritus and viruses).

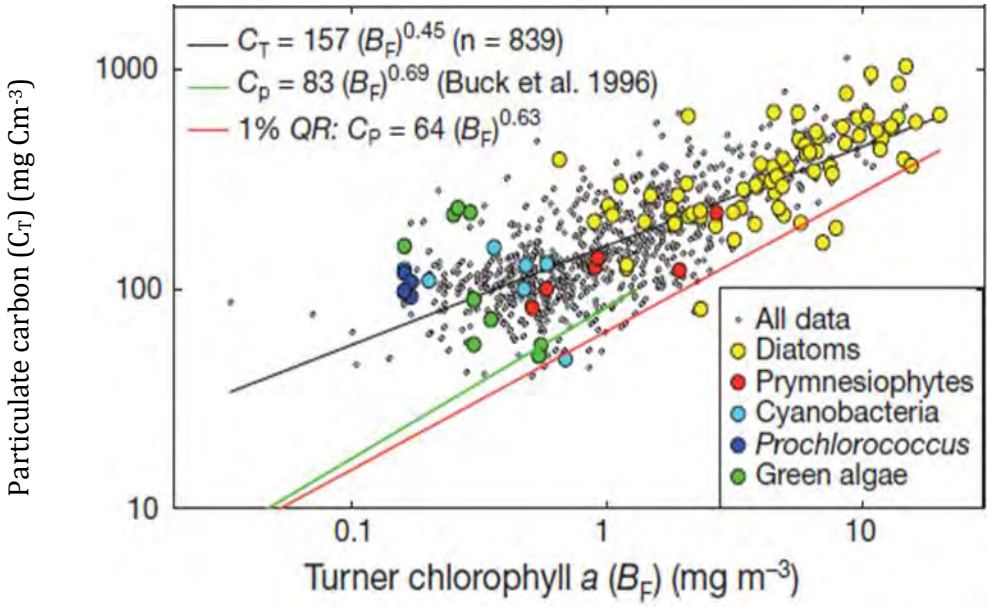


**Figure 4.7** Particulate carbon ($C_T$) as a function of chlorophyll *a* for offshore data. Chlorophyll *a* Least-squares fits to log-transformed data are shown as solid black line, as well as minimum carbon estimates (*C*p, by quantile regression [QR] $q$ = 0.01) as the solid red line which may be interpreted as the upper limits for phytoplankton carbon in the system. The solid green line represents the relationship between phytoplankton carbon and chlorophyll from field data by Buck *et al.,* (1996) for comparison. Figure taken from

The S09 method was applied to co-located POC and chl-a data from both surface underway and profile CTD samples collected on all cruises listed in Table 1. A 1% quantile regression was fitted to the log-transformed data as shown as above (see Figure 4.8) to derive the following equation for converting chlorophyll into $C_{phyto}$.

**S09 $C_{phyto}$ = 42 (chl) $^{0.85}$ (7)**

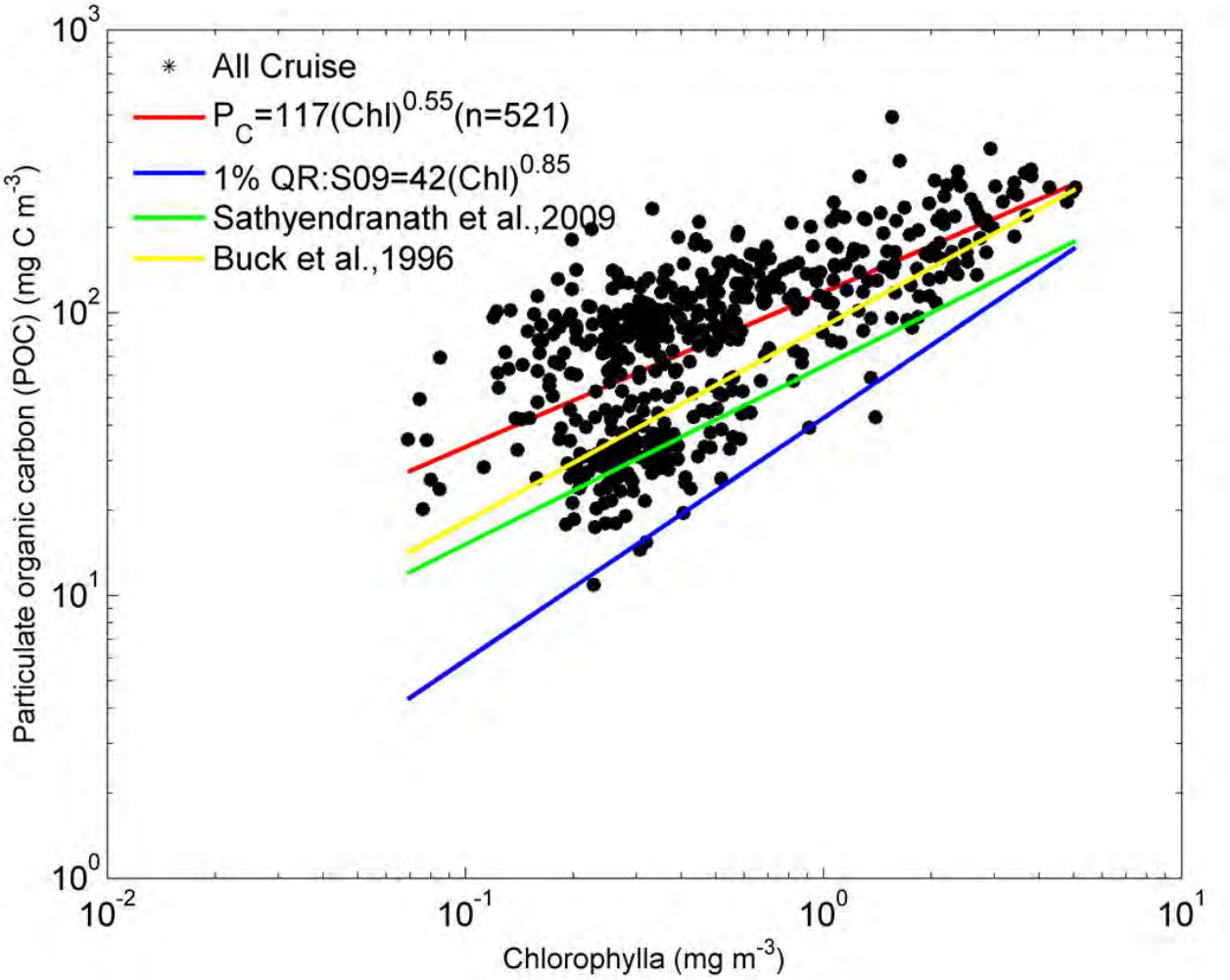


**Figure 4.8** POC as a function of chlorophyll for all cruise data. The least-square fits to log-transformed data are shown in red, as well as minimum carbon estimates by quantile regression [QR] (q=0.01), in dark blue which can be interpreted as the value below which phytoplankton carbon can occur in the system. The relationship between phytoplankton carbon and chlorophyll from Sathyendranath *et al.,* (2009) (green line) and Buck *et al.,* (1996) (yellow line) are also shown for comparison.

# 5. Results

## 5.1 Seasonal evolution of phytoplankton biomass

The time evolution of physical and biogeochemical properties along the glider section has been previously presented by Swart *et al.,* (2014) and Thomalla *et al.,* (submitted), to highlight the substantial seasonal changes in chlorophyll (Fig. 5.1a). Low chlorophyll (<0.4 mg $m^{-3}$) concentrations were found at the beginning of October to late October which coincided with deep MLD's (down to 200 m). The deep MLD's are likely driven by a combined effect of winter wind stress and reduced buoyancy due to lower solar heating. The occurrence of weak stratification in spring and the presence of mesoscale to sub-mesoscale eddies led to variability in the horizontal distribution of stratification that is expressed in the sudden variation of MLD (Swart *et al.,* 2014). The shoaling of the MLD from ~100 - 20 m in late November sees a concomitant increase (>0.55 mg $m^{-3}$) in surface chlorophyll (Fig. 5.1a) that was sustained throughout summer until the end of the sampling in February. The highest chlorophyll concentration was observed in mid-December which occurred with the persistence of shallower MLD's.

Overall, there is a rather good visual correspondence between chlorophyll and POC evolution (Fig 5.1b) supporting the results shown by Swart *et al.,* (2014) for chlorophyll. This implies that there is a relationship between chlorophyll and POC even if some differences are visible. The POC data were calculated by applying equation (3) to the glider $b_{bp}$ 470 data. The lowest concentrations (50 – 80 mg C $m^{-3}$) were found in October, increasing in November (~80 – 120 mg C $m^{-3}$) and highest concentrations extending from December through to February (80 – 150 mg C $m^{-3}$).

Major differences in biomass distribution between chlorophyll and POC are evident in late September / early October when deep MLD's (~150 m) coincide with higher homogenous POC concentrations relative to chlorophyll.

Other differences are evident in early October when a higher patch of POC (~ 80 mg C $m^{-3}$) was not observed in the chlorophyll measurement. Conversely, in the first week of January high chlorophyll does not translate to similarly high POC. From mid-January until the end of the sampling period chlorophyll presented more short term variability than the one observed in POC.

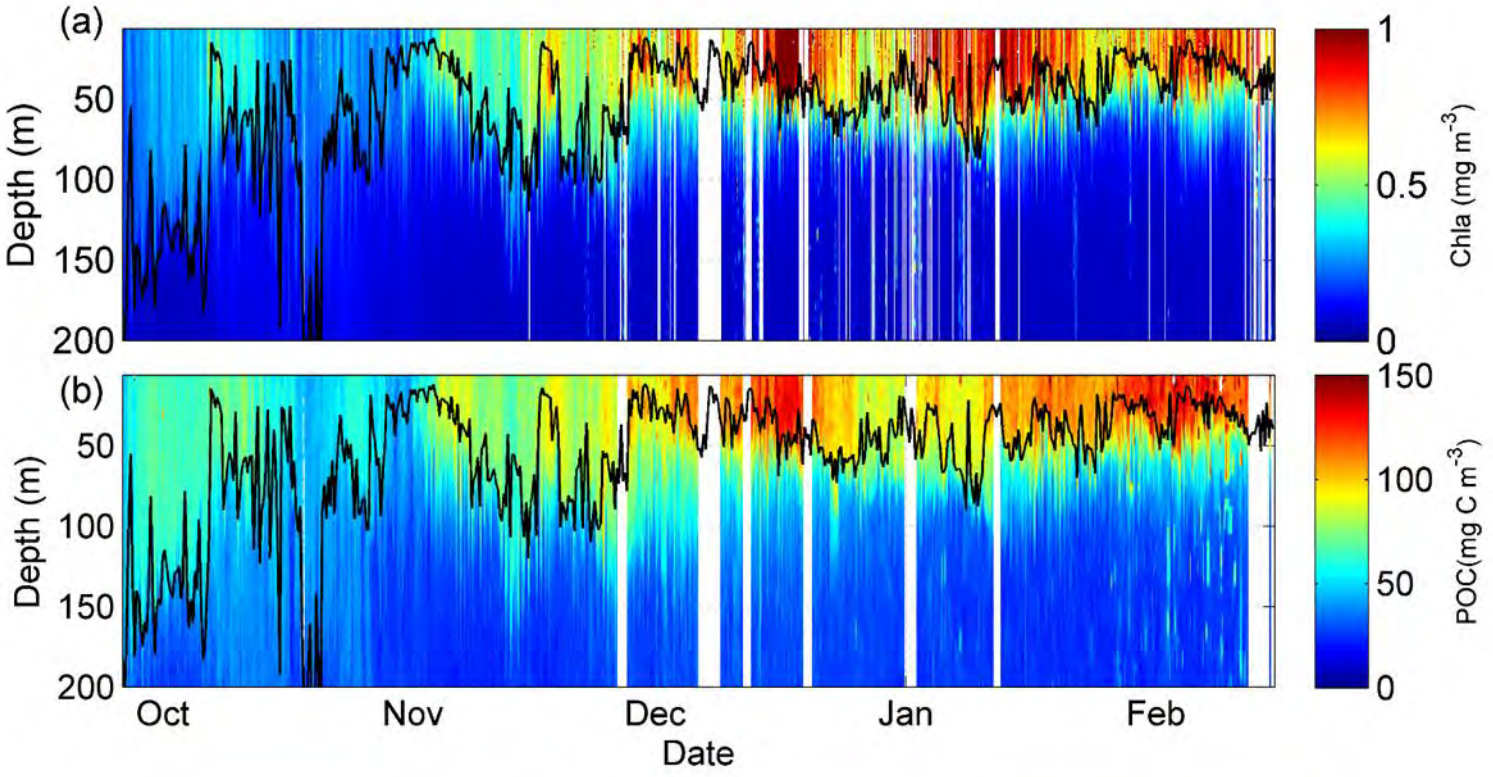


**Figure 5.1.** Section plot of (a) chlorophyll and (b) particulate organic carbon (constructed from equation 3)

## 5.2 Comparing the methods to derive phytoplankton carbon

When applied to the glider $b_{bp}$ and chlorophyll data, 3 of the different methods of retrieving phytoplankton carbon described in section 4 show similar results (Figure 5.2a, b and d). In particular the methods 30%POC (Figure 5.2a) and B05 (Figure 5.2b) show almost identical distribution patterns with concentrations that range between (0 and 45 mg C $m^{-3}$). Similarly, the method of S09 (Figure 5.2d), the only method that uses chlorophyll rather than particulate backscattering to retrieve phytoplankton carbon, shows surprisingly similar results to the methods of B05 and 30% POC.

The major differences are that S09 produces slightly lower concentrations in late September and early October (during the period of deepest mixed layers) and at the end of the glider transect in early February. While slightly higher peaks in $C_{phyto}$ were evident in the S09 method on occasions during the summer, most notably the peak in mid-December. For the month of January to mid-January, the 30%POC and B05 methods show lower $C_{phyto}$ compared to S09.

The values of $C_{phyto}$ that showed the most different results were from the M13 method (Figure 5.2 c) which overall produced much larger values of $C_{phyto}$ (range 0 - 80 mg C $m^{-3}$). In this method ~ 30 - 40 mg C $m^{-3}$ was found in October compared to the other three methods that was closer to ~20 mg C $m^{-3}$. Similarly, from November to February $C_{phyto}$ from M13 ranged from ~40 – 80 mg C $m^{-3}$ compared with ~ 20 - 50 mg C $mg^{-3}$ in the other three methods. Two patches of similar $C_{phyto}$ concentration were found in mid-October (when MLD's were deepest) and first week of November (after rapid MLD shoaling) when all four methods produced similar low $C_{phyto}$ concentrations of < 20 mg C $m^{-3}$.

The white area in M13 (Figure 5.2 c) represents backscattering $b_{bp}$ values from our glider data that fell below the limit of applicability of equation (6). The large intercept of equation (6) meant that a large number was subtracted from the glider $b_{bp}$ such that when backscattering was low, applying equation (6) resulted in negative values which were converted to missing numbers. It should be noted that these $b_{bp}$ value fell below the point where the slope crosses the y intercept (Fig. 4.6).

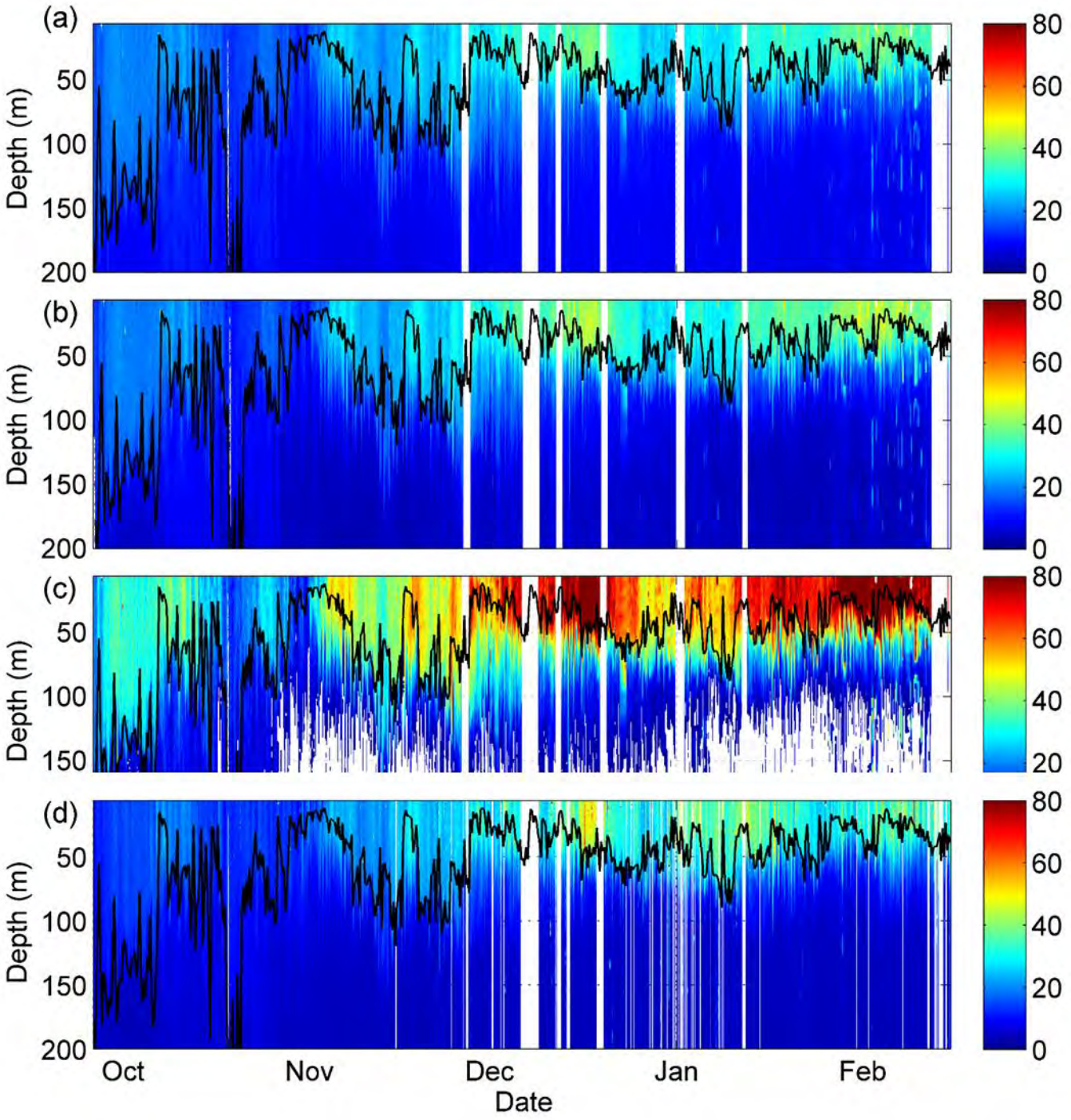


**Figure 5.2.** Section plot of phytoplankton carbon ($C_{phyto}$ mg C $m^{-3}$) along the glider transect using backscattering ($b_{bp}$) at 470nm according to (a) the 30% POC method of deriving phytoplankton carbon; (b) the Behrenfeld *et al.,* 2005 (B05) backscattering ($b_{bp}$) method; (c) the Martinez-Vicentez *et al.,* 2013 (M13) method and (d) Sathyendranath *et al.,* 2009 (S09) method of deriving phytoplankton carbon from chlorophyll. MLD is overlaid in black

## 5.3 Comparison of chlorophyll and phytoplankton carbon time series with depth.

A comparison of the different methods of detecting $C_{phyto}$ with depth (Figure 5.4) shows that discrepancy between M13 and the three other methods decreases with depth. This indicates that there may be a dependence of the different methods on depth which may be driven by phytoplankton concentration. A comparison of the chlorophyll concentration (an alternative estimate of phytoplankton biomass) with depth (Figure 5.3) indeed shows that chlorophyll concentration at 80 m are much lower than at the sub-surface (10 and 40 m). The difference between M13 and the other three methods thus decreases when phytoplankton biomass is low (~0.25 mg C $m^{-3}$) e.g., at depth (80 m) and from mid-October to the beginning of November, when surface chlorophyll concentrations are low (Figure 5.3) and all four methods of $C_{phyto}$ tend to converge (Fig. 5.3a, b & c). Since uncertainties in the different methods can result from discrepancies in both magnitude (e.g. M13 gives higher $C_{phyto}$ concentration at higher biomass) and temporal variability (e.g. one method may give a different indication of temporal variability in biomass) the $C_{phyto}$ results were correlated with chlorophyll as an independent measure of phytoplankton biomass variation (see Table 2 for $r^2$ correlation coefficient).

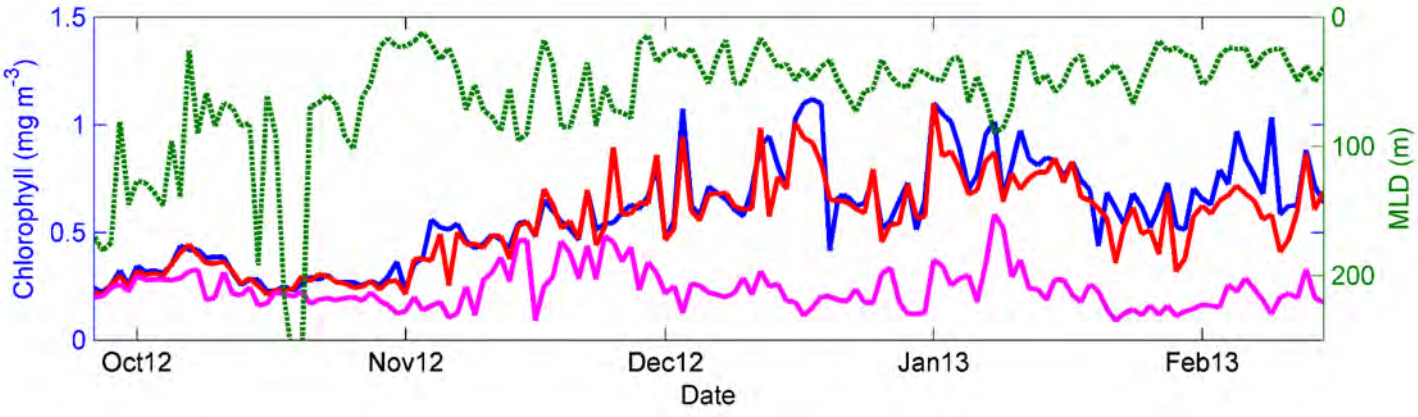


**Figure 5.3.** Chlorophyll distribution at different depth with MLD. 10 m (blue), 40 m (red) and 80 m (magnate). MLD overlaid in green.

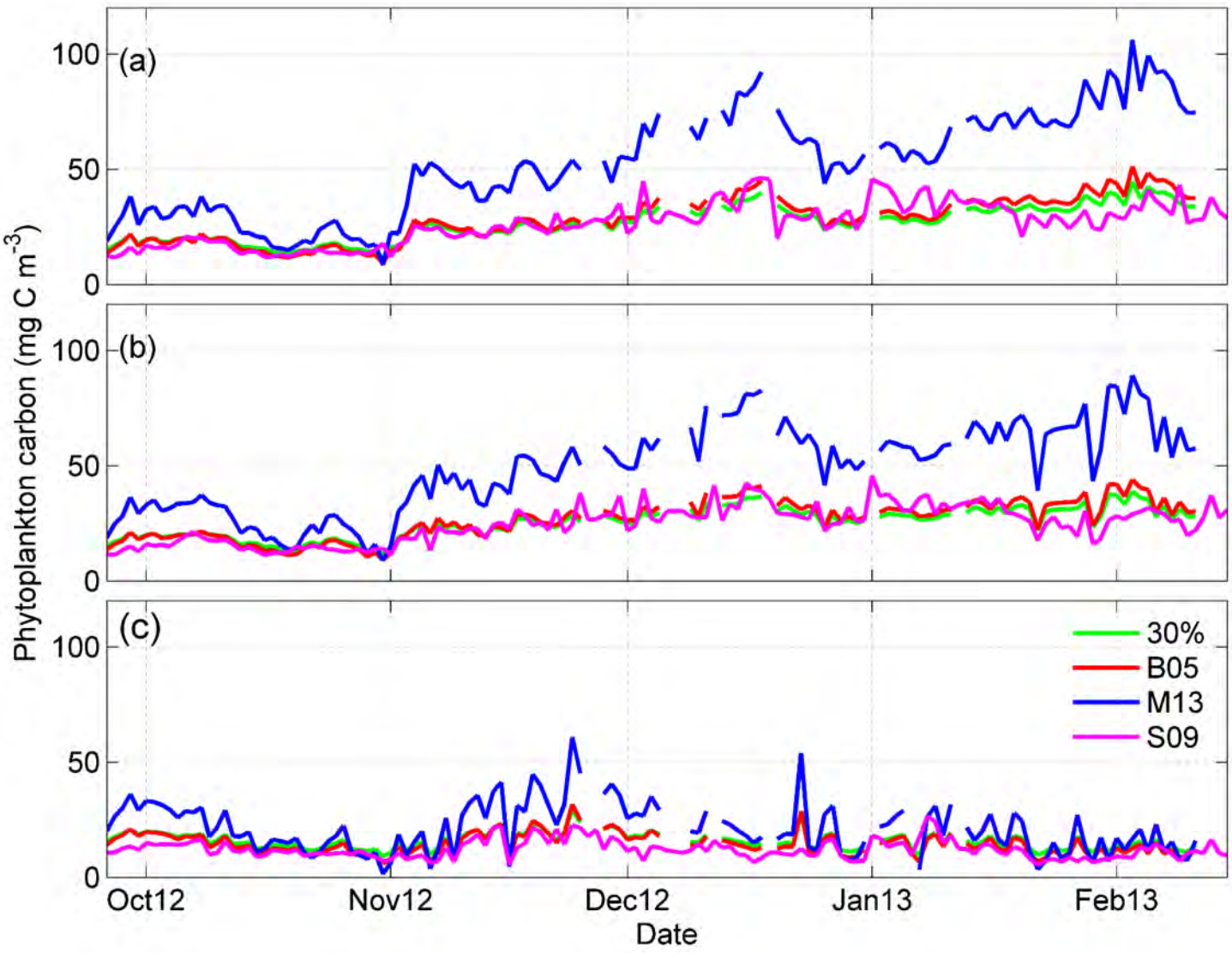


**Figure 5.4.** Temporal and depth distribution of phytoplankton carbon ($C_{phyto}$) at different depth (A) 10 m, (B) 40 m and (C) 80 m.

The similar correlations between chlorophyll and $C_{phyto}$ for all three methods (M13, B05, 30%POC) mean that there is no discernable temporal bias in any of the methods. Despite $C_{phyto}$ from M13 being more similar in magnitude to B05, S09 and 30%POC at depth (80 m) (and lower biomass), the correlations between chlorophyll and $C_{phyto}$ decrease with depth for all three methods ( M13, B05 and 30%POC) from $r^2 = 0.63$ at 10 m to $r^2 = 0.53$ at 80 m. The decrease in correlation with depth is likely driven by physiological changes in phytoplankton carbon to chlorophyll ratios with depth that are not driven by biomass.

**Table 2. The correlation coefficients ($r^2$) of the linear regression of chlorophyll at different depths together with the slope of the linear correlations**

| | Chl-a @ Depth | | | Slope @ Depth | | |
|---|---|---|---|---|---|---|
| | | | | | | |
| $C_{phyto}$ Method | 10 m | 40 m | 80 m | 10 m | 40 m | 80 m |
| 30 % | 0.63 | 0.64 | 0.53 | 26.48 | 25.97 | 28.25 |
| B05 | 0.63 | 0.63 | 0.53 | 33.75 | 33.1 | 36.0 |
| M13 | 0.63 | 0.64 | 0.53 | 78.14 | 76.64 | 83.12 |
| S09 | 0.99 | 0.99 | 0.99 | 38.72 | 39.26 | 43.53 |

## 5.4. Changes in ratio of $C_{phyto}$ to chlorophyll with depth

Given that chlorophyll and $C_{phyto}$ are both indicators of phytoplankton biomass it is not surprising that they are positively correlated (i.e., an increase in $C_{phyto}$ is observed with an increase in chlorophyll (Fig. 5.5). What is interesting to note is how the relationship varies with depth. As the depth increases from 10 m to 80 m the correlation between $C_{phyto}$ and chlorophyll reduces (from $r^2$ =0.63 to 0.53; see Table 2) showing that the relationship between $C_{phyto}$ to chlorophyll is depth dependent. Since S09 method of generating $C_{phyto}$ is derived from chlorophyll the relationship between chlorophyll and $C_{phyto}$ can be seen to be linear and constant with no discernible variability with depth or chlorophyll concentration.

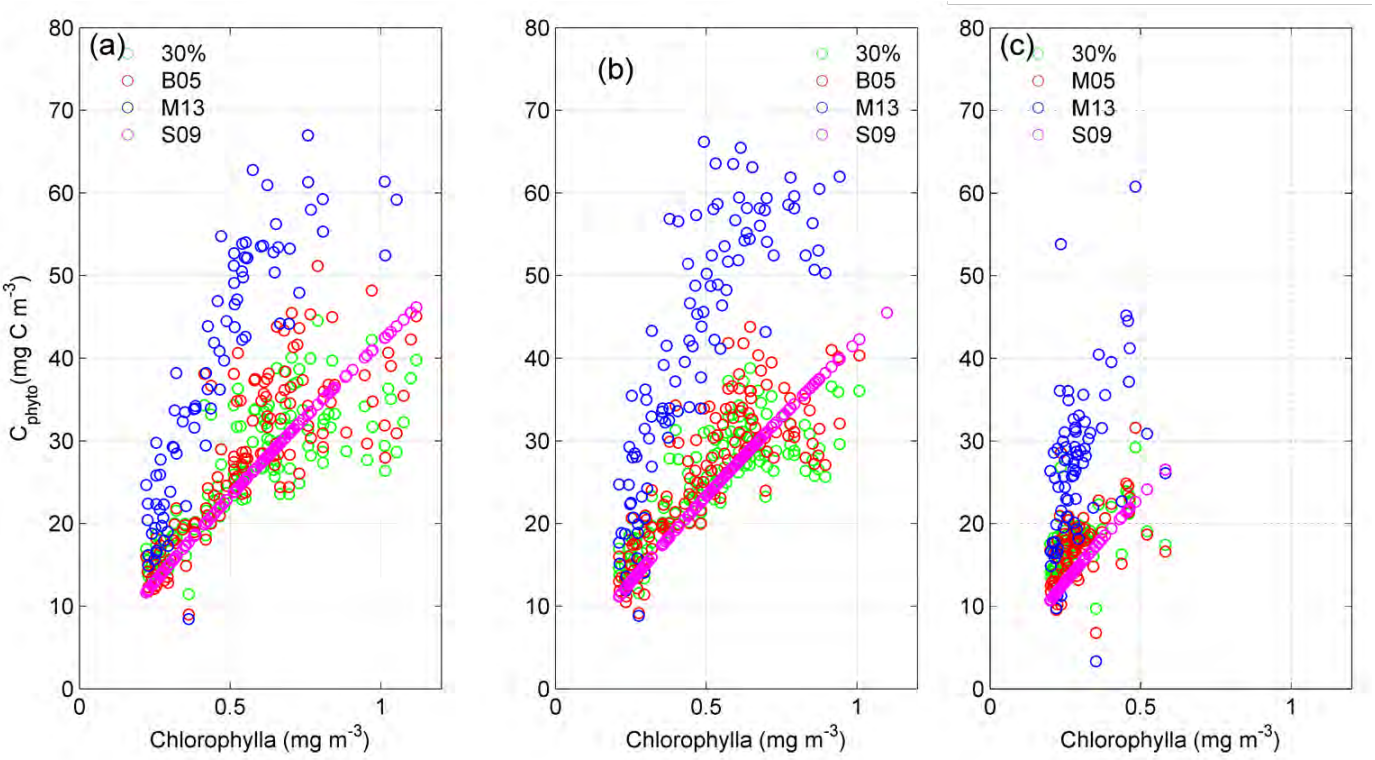


**Figure 5.5.** Variation of surface phytoplankton carbon ($C_{phyto}$) and chlorophyll with depth (A) at 10 m, (B) 40 m and (C) 80 m. The chlorophyll match the $C_{phyto}$ at the same depth.

The 30%POC and B05 methods of generating $C_{phyto}$ clusters around S09 (i.e. shows a similar slope) but with more spread through variability in $C_{phyto}$:chl-*a* ratio. M13 on the other hand has a much larger $C_{phyto}$ concentration per unit of measured chlorophyll and a much steeper slope. The 30%POC, B05 and M13 $C_{phyto}$ methods all show highest variability in $C_{phyto}$ distribution to chlorophyll when chlorophyll concentrations are high (>0.5 mg $m^{-3}$). The higher $C_{phyto}$:chl-*a* ratios of M13 is driven by the higher $C_{phyto}$ value relative to the other methods. For all methods there is an increase in the slope (Table 2) of the correlation with depth (the slope is steeper at 80 m than the surface). This implies that for the same amount of chlorophylla the coincident amount of $C_{phyto}$ increases with depth. i.e., at depth there is more $C_{phyto}$ relative to chlorophyll than at the surface.

## 5.5. Seasonal changes of Chlorophyll to $C_{phyto}$ ratio

The seasonal evolution of the chl-*a*:$C_{phyto}$ ratio computed for the different methods is shown in Figure. 5.6. The high Chl-*a*:$C_{phyto}$ ratios in red in the M13 section at depth marks the point in the data set where $C_{phyto}$ values approach zero driving unrealistic high chl-*a*:$C_{phyto}$ ratios. A comparison of the different chl-*a*:$C_{phyto}$ sections for each method shows very low ratios at the surface with the M13 method. These low ratios are driven by the high $C_{phyto}$ values of M13 relative to other methods, particularly when the biomass is high at the surface. An exception is during the episodic event in late October where high chl-*a*:$C_{phyto}$ ratios are seen in M13 (>0.03) similar to those found in the 30%POC and B05 methods. The B05 and 30%POC methods show very similar chl-*a*:$C_{phyto}$ ratios (as expected from their similar $C_{phyto}$ distributions seen in Figure 5.2) however with B05 , higher chl:$C_{phyto}$ ratios (~0.02) can be seen to occur below the MLD ( ~200 m) from mid-October to mid-November and also from January to February (Fig. 5.6a & b).

By construction, S09 has a tight constrain in the chl-*a*:$C_{phyto}$ ratio due to the quantile relationship that derived $C_{phyto}$ from chlorophyll in section 4 ; as such Fig.5.6d shows a lower range of variability in chl-a:$C_{phyto}$ ratios with a maximum of ~0.025 mg $m^{-3}$ and a minimum of ~0.02 mg $m^{-3}$ with a moderate change with depth and less seasonal variability (see Sec.5.4). In general, chl-*a*:$C_{phyto}$ ratios tended to be lower in October when mixed layers were deep, increasing towards summer with increasing concentrations of phytoplankton biomass (Fig. 5.6). The higher variation in chl-*a*:$C_{phyto}$ ratios during the bloom from November through to February obtained with the backscattering methods point towards physiological

(cellular packaging) or ecological (e.g. community structure) adjustments in the proportion of carbon to chlorophyll per cell.

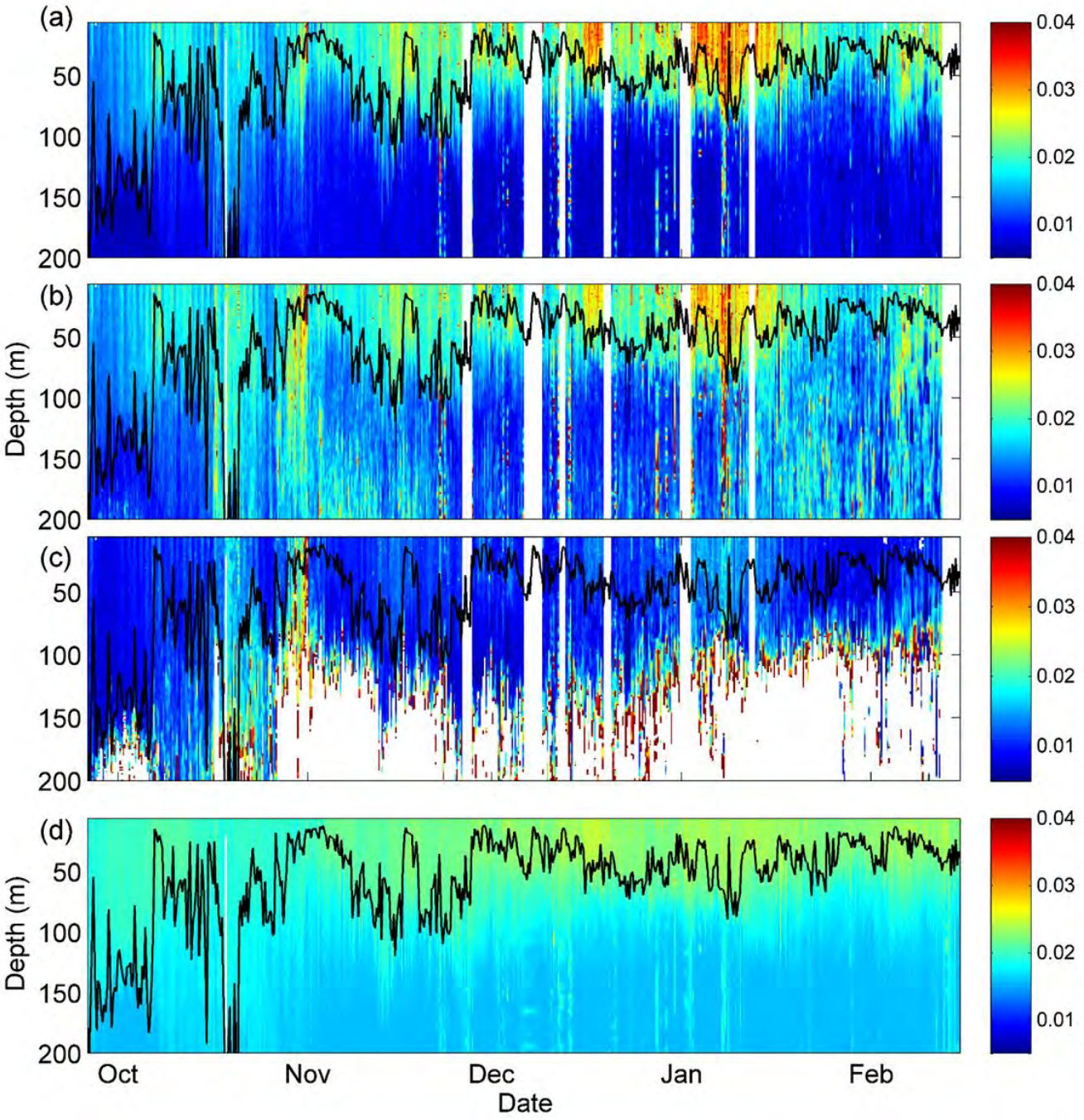


**Figure 5.6.** Section plot of Chl-*a*:$C_{phyto}$ along the glider transect using different methods of deriving phytoplankton carbon (a) 30% POC method (b) Behrenfeld *et al.,* 2005 (B05) method (c) Martinez-Vicentez *et al.,* 2013 (M13) method and (d)using Sathyendranath *et al.,* 2009 (S09) method. MLD overlaid in black.

# 6. Discussion

This study uses a high resolution glider data set from the Southern Ocean to compute phytoplankton carbon ($C_{phyto}$) using four different methods available in the literature. The ability to get a good estimate of $C_{phyto}$ is very important as it provides an estimate of biomass that is core to estimating net primary productivity (in mg C $m^{-3}$), a key measurement of ecosystem health and carbon cycling. In addition, good measurement of $C_{phyto}$ enable us to better understand changes in cellular carbon to chlorophyll ratios, which provides information on phytoplankton physiology (e.g., cellular adjustments to changes in light, temperature and nutrients (Behrenfeld *et al.,* 2005). Deriving a good estimate would enable us to refine models of phytoplankton dynamics (Sathyendranath *et al.,* 2009). Since the biological pump in the Southern Ocean drives 33% of global organic carbon flux (Schlitzer, 2002), it is necessary to improve our understanding of the response of the Southern Ocean biological pump to climate change associated with increased anthropogenic carbon fluxes. For this, improved estimates of $C_{phyto}$ and their varying relationship to chlorophyll is necessary.

The 30%POC, B05 and M13 methods used in this study make use of particulate backscattering ($b_{bp}$), while the S09 uses chlorophyll to derive $C_{phyto.}$ Although these four methods are being compared in this study, it should be noted that these are not the only methods available to derive $C_{phyto}$ but they are the most widely used.

## 6.1. Comparing the different methods of deriving phytoplankton carbon

It should be noted that the aim of this study is not to assess the quality and merit of the single individual methods against each other but rather, to evaluate the differences and implication of the various methods so that informed decisions can be made when choosing to apply one method over the other. It should also be noted that the different methods used in this research were derived from data, which were obtained from different oceanic regions. For example, the M13 equation was derived from *in situ* data from the Atlantic, the S09 equation from *in situ* data from the NW Atlantic, the B05 equation from using global satellite data, and the 30%POC method from in *situ* data from the Southern Ocean. Despite regional differences in their origins, all equation have been applied to glider transect in the Sub Antarctic Southern Ocean and as such differences can be expected.

The most evident result from the comparison of the different methods is that the 30% POC, B05 and S09 methods show a much more similar pattern and range in phytoplankton distribution when compared to M13 (Fig. 5.2a, b and d). The M13 method derives much higher concentrations of $C_{phyto}$ and seems to overestimate $C_{phyto}$ when compared to the other methods. The difference is exaggerated when chlorophyll concentration are high as evidenced in the convergence of the different methods when chlorophyll concentration are low (< 0.025mg $m^{-3}$) e.g., at depth and in the month of October (Figure 5.4). The reason for the higher $C_{phyto}$ estimates using M13 is the steep slope of equation 6; see Figure 5.2 c. The slope of M13 is much steeper, approximately double the slope used for B05 (Figure 4.6) and 30%POC (Figure 4.4). As such, high values of particulate backscattering will produce much higher values of $C_{phyto}$ when equation 6 is applied to the data set relative to the 30%POC and

B05 methods. In the discussion of Martinez-Vicente *et al.,* (2013), the possible explanation proposed for the doubling of parameters between their equation (M13) and that of Behrenfeld *et al.,* (2005) was "uncertainties in satellite and *in situ* estimates of $b_{bp}$ and /or differences in the spatio-temporal scales of the two studies".

In addition, differences may be driven by the fact that equation (6) from Martinez-Vicente *et al.,* (2013) was generated from *in situ* $b_{bp}$ data from the low biomass Atlantic which was less than $0.003 m^{-1}$. The eight data points that exceeded this threshold showed a shift in the relationship that was not possible to describe with a single linear function. Despite being generated with $b_{bp}$ data $<0.003 m^{-1}$, this equation was applied to all glider $b_{bp}$ data from ($0.001\ m^{-1}$ – $0.01\ m^{-1}$) even if they potentially fell above the threshold of applicability of equation (6). In addition, the application of the of the M13 method to our glider data set resulted in lots of negatives values (which were converted to missing values). This is due to our low $b_{bp}$ values that fell below the threshold of the data used to generate equation (6), which resulted in negatives values when the threshold of the data used to generate equation (6) was subtracted from the $b_{bp}$ values (observed as white area in Fig.5.2 c). It is thus possible that the overestimated $C_{phyto}$ concentration (and negative values at low $b_{bp}$) generated from this method are the result of unsuitable application of a regionally derived model. The 30%POC and B05 methods on the other hand were derived from field data obtained from the Southern Ocean (30%POC) and remote sensing which incorporates all oceanic region (B05).

All four methods tend to show greater similarity in $C_{phyto}$ biomass distribution when chlorophyll concentration are low (i.e., in spring and at depth; Fig 5.2a, b, c and d). Thus when chlorophyll biomass is low (<0.25 mg $m^{-3}$) it makes little difference which method of estimating $C_{phyto}$ is used. Despite their different origins, the two remaining methods for estimating $C_{phyto}$ based on $b_{bp}$ (30%POC and B05) are considerably close to the result obtained by Sathyendranath *et al.,* (2009) that is based on chlorophyll. However, the 30%POC and B05 results shows that there is close-fitting of phytoplankton carbon to S09 at lower chlorophyll concentrations and that $C_{phyto}$ are more scattered at high chlorophyll concentrations (Fig. 5.5). By definition, the S09 method shows very little variation of $C_{phyto}$ with chlorophyll concentration or depth (Fig. 5.5). This is due to the fixed 1% quantile regression that was applied to our data, which represents the upper limit of $C_{phyto}$ in the system. The implication of this is that the S09 method does not allow for a scenario where $C_{phyto}$ does not increase without a corresponding increase in chlorophyll (and vice versa). The variability (scatter) noticed in B05 and 30%POC results (Fig. 5.5) may be connected to changes in community structure in response to nutrients limitation or the acclimation to variable light (Sathyendranath *et al.,* 2009).

## 6.2. Impact of environmental conditions on the chlorophyll and $C_{phyto}$ ratio

Depth (and MLD) plays a crucial role in determining the amount of $C_{phyto}$ relative to carbon in phytoplankton cells as adjustments in depth (and MLD) influence both light and nutrient availability. Depth thus influences phytoplankton biomass and community (Jager *et al.,* 2008). In the euphotic zone the complicated effect of temperature, nutrients and light on phytoplankton can result in a non-linear relationship between phytoplankton chl-*a* concentration and carbon biomass with change in depth (Geider *et al.,* 1997; Behrenfeld and Boss 2003; Armstrong, 2006).

There has been previous studies which suggested that chl-*a*:$C_{phyto}$ ratio would be low at maximum light conditions, decrease with temperature and nutrients concentrations and would peak at minimum light conditions and increased temperature and nutrient stock (Geider *et al.,* 1997; Taylor *et al.,* 1997; Socal *et al.*, 1999; Behrenfeld *et al.,* 2005, Lu *et al.,* 2009). The reason is that as light decreases with depth phytoplankton increase their cellular chlorophyll concentration to be able to adapt to their low light conditions (Behrenfeld and Boss, 2003). In the presence of low light phytoplankton tend to increase the volume of chlorophyll packed into their cells, thereby increasing their light harvesting ability (Behrenfeld and Milligan, 2013). In (Fig. 5.5) we anticipated a change in $C_{phyto}$:chl-*a* through chlorophyll packaging by the cell and a subsequent decrease in slope with increase in depth. However, this was not the case and in fact a slight increase in the slope of $C_{phyto}$:chl-*a* ratio was observed (Table 2). It should be noted that we increased the highest depth used in this study from 80 to 120 m (see appendix), this is in line with previous research that said that below 100 m living cells are unlikely to be found (Geider *et al.,* 1998).

However at the depth of 120 m the slope was even steeper than the chosen depth of 80 m used in this study. The observed increase in slope with depth observed with the M13 method is likely a methodological artefact (and not a physiological one) driven by the unrealistically high chl-*a*:$C_{phyto}$ ratios observed at depth in the M13 section (Figure 5.6c) that were driven by $C_{phyto}$ values which approached zero. S09 method was developed using data from depth less than 40 m .A possible reason for the absence of decrease in slope with depth is that the Southern Ocean is well mixed due to strong winds that drive overturning circulations that move water from the deep to the surface. This process leads to the mixing of phytoplankton from the surface to below 80 m, thereby leading to a physiological adaptation of the phytoplankton to the overall mean light environment of the entire depth range. Hence there is little relationship observed with change in slope of the chl-*a*:$C_{phyto}$ with depth.

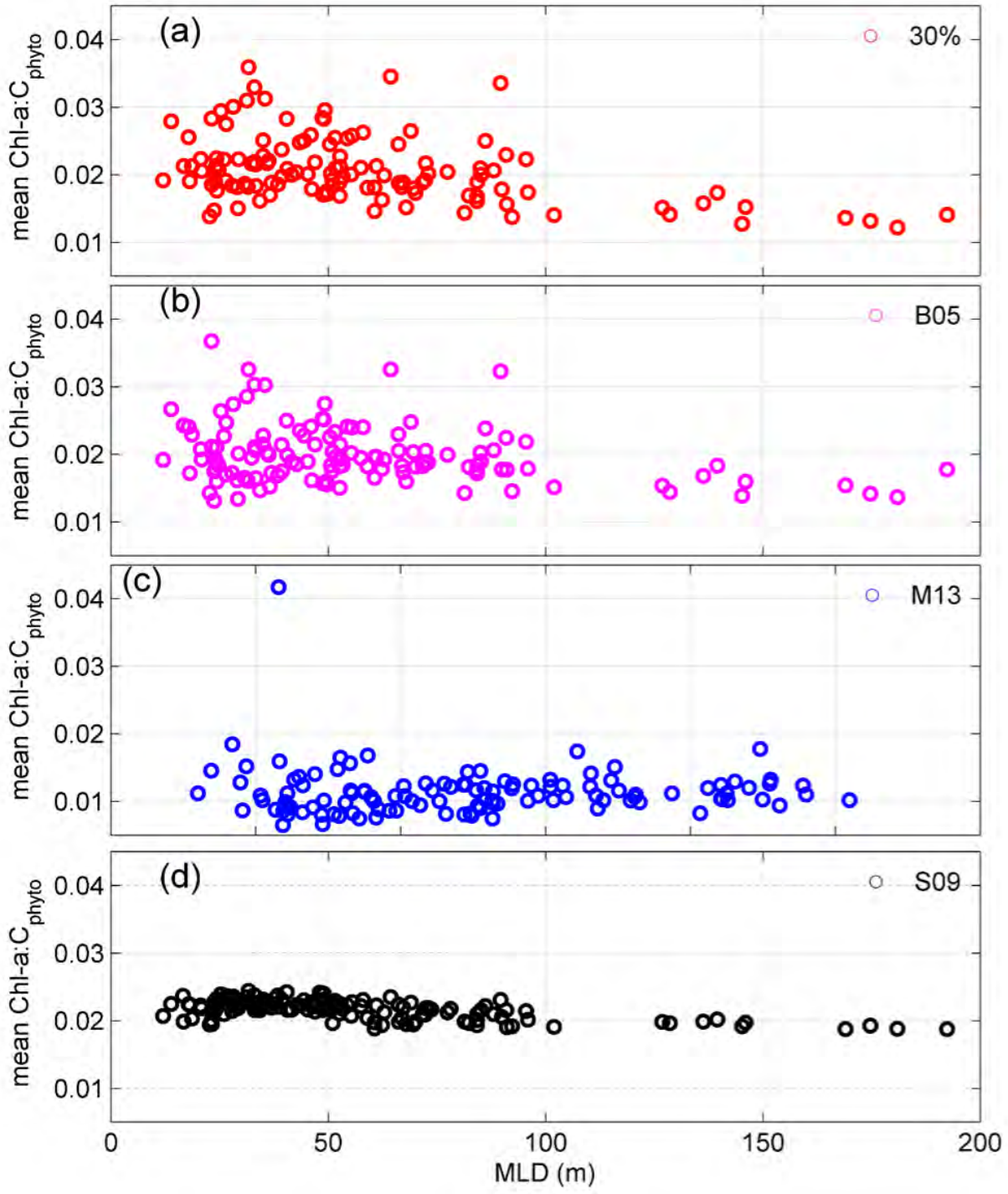


**Figure 6.1.** Mean chl-*a*:$C_{phyto}$ in MLD against MLD

Although chl-*a*:$C_{phyto}$ did not decrease with depth due to physiological adaptation to mean light exposure in the well mixed Southern Ocean, it is possible that a relationship would exist between chl-*a*:$C_{phyto}$ ratios and MLD as a deep MLD would result in a low mean light exposure than a shallow MLD. The mean chl-*a*:$C_{phyto}$ ratio in the MLD was plotted against MLD to investigate whether deep MLD's (low mean light ) drove high chl:Cphyto ratios through physiological adaptations of chlorophyll packaging. However, no strong relationship was observed (Figure 6.1) and the highest chl-*a*:$C_{phyto}$ ratio were not found at the deepest MLD (i.e., lowest mean light).

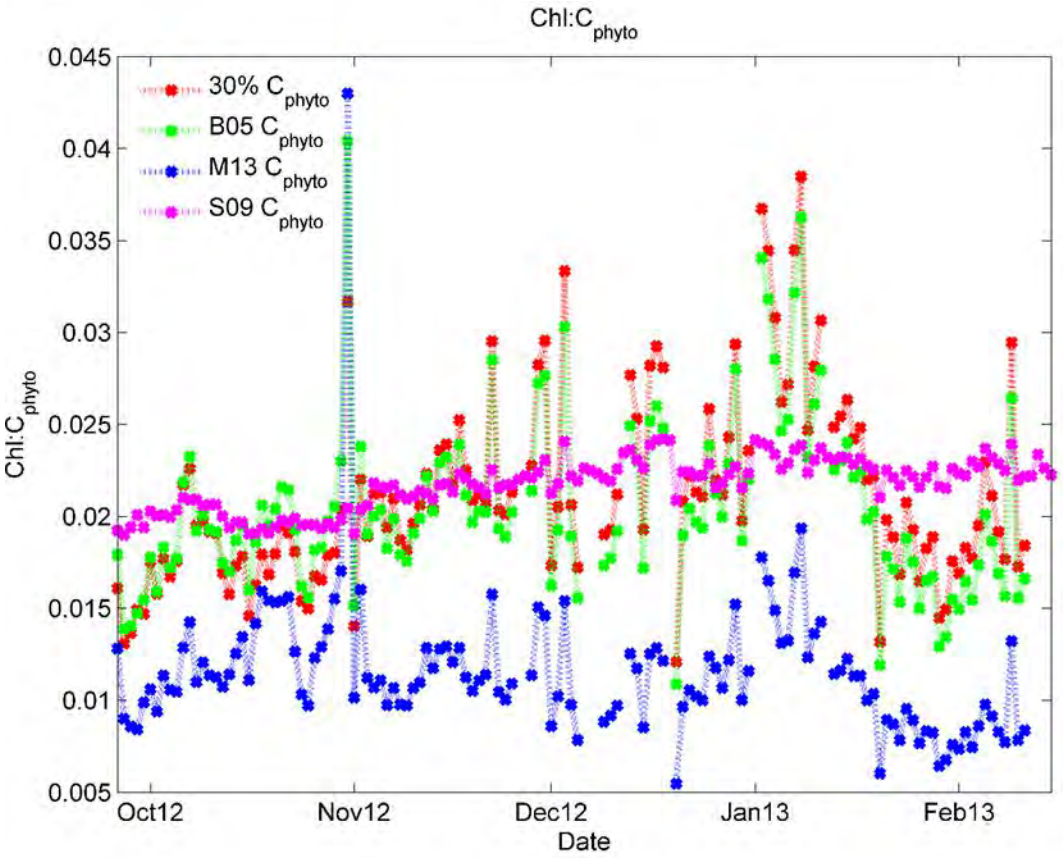


**Figure 6.2.** Temporal surface variation of chlorophyll and phytoplankton carbon ($C_{phyto}$) ratio.

Although the variability in the chl-*a*:$C_{phyto}$ ratios are driven by light when MLD changes, there are many other factors also influencing chl-a:$C_{phyto}$ such as iron availability, physiology, previous light history etc., such that it is not only MLD that drives changes in chla:$C_{phyto}$ hence the lack of strong relationship. For example, Sathyendranath *et al.,* (2009) suggested that $C_{phyto}$:chl-*a* ratios would be lowest when larger diatoms are present and be highest when smaller species e.g., *Prochlorococcus sp* are present. Some of the variability observed in chl-*a*:$C_{phyto}$ ratios (particularly at high chlorophyll concentrations) could thus be the result of different sized species dominating the community structure at different times.

It is also important to remark here that some co-variations of the chl:$C_{phyto}$ ratio may be due to the correction method that was applied to surface chlorophyll to remove the quenching effect (see section 4.3.1). Similarly, previous studies have shown, that the range of chl-*a*:$C_{phyto}$ ratios observed in the Southern ocean are the result of seasonal variation in the phytoplankton response to light and nutrient limitation from spring to summer (Behrenfeld *et al.,* 2005). The different methods respond in similar way by moving from typically low to high ratios in the spring ( when iron concentrations are high and light is lower ) to high ratios in the summer (when light is high and iron concentration are typically low). The episodic event of high chl-*a*:$C_{phyto}$ that was observed in the first week of November (Fig. 6.2) was the result of low $b_{bp}$ which creates a low $C_{phyto}$ thereby resulting in a high chl-*a*:$C_{phyto}$ ratio in all three $b_{bp}$ methods of deriving $C_{phyto}$. The higher chl-*a*:$C_{phyto}$ ratios observed below the MLD (Fig. 5.6b) in the B05 method which was absent in 30%POC (Fig. 5.6a) was the result of the B05 method which drives lower $C_{phyto}$ value relative to the 30%POC method when $b_{bp}$ is low. This in turn drives high chl-*a*:$C_{phyto}$ ratio in the B05 method at depth (Figure 5.6b).

A plot of the surface chl-*a*:$C_{phyto}$ ratios derived from the four different methods provides a temporal display of the variability in M13 chl-*a*:$C_{phyto}$ ratios with time. The M13 chl-*a*:$C_{phyto}$ ratios were half that of the 30%POC, B05 and S09 methods due to the high $C_{phyto}$ concentrations this method produces. However, the range of variability is very similar to the other $b_{bp}$ derived methods (30%POC and B05). The S09 method shows a very similar mean range of range of chl-*a*:$C_{phyto}$ ratios as the B05 and 30%POC but the range of variability is much lower. The low range of variability in S09 compared to 30% of POC, B05 and M13 (Fig.6.2) is driven by the fact that $C_{phyto}$ in this method is derived from the quantile regression with chl and hence there is no possibility for additional drivers of variability to influence chl-*a*:$C_{phyto}$ ratios (e.g. physiology, community structure, packaging) Sathyendranath *et al.,* (2009)

## 7. Conclusion

This study used a high-resolution optical data from glider measurement in the SAZ to compare the different empirical estimates of phytoplankton carbon from the literature. The methods are the backscattering based method and the chlorophyll based method. The application of the different methods on our data resulted in different magnitude of $C_{phyto}$. Out of the four method used 3 (30%POC, B05 and S09) showed similar $C_{phyto}$ which we considered are within the reasonable range of estimation according to previous studies (see section 4).

The M13 method derived much higher concentrations of $C_{phyto}$ and seems to overestimate $C_{phyto}$ when compared to the other methods particularly when chlorophyll concentrations are high. This overestimation is likely driven by the fact that the M13 method was generated from *in situ* $b_{bp}$ data from the low biomass Atlantic. It is thus possible that the overestimated $C_{phyto}$ (and negative values at low $b_{bp}$) generated from M13 are the result of unsuitable application of a regionally derived model. However, all four methods tend to show greater similarity in $C_{phyto}$ biomass distribution when chlorophyll concentration are low (i.e., in spring and at depth). Thus when chlorophyll biomass is low (<0.25 mg $m^{-3}$) all four methods performed well at estimating $C_{phyto}$.

Although the chla:$C_{phyto}$ ratios of M13 were lower (due to overestimated $C_{phyto}$), their range of variability was very similar to B05 and 30%POC methods accounting for potential adjustments in cellular packaging relating to nutrient stress, light availability and community structure . The S09 chla:$C_{phyto}$ ratios on the other hand has a similar magnitude to B05 and 30%POC but the variability was much lower as this method does not allow for

adjustments in $C_{phyto}$ without proportional changes in chlorophyll and hence cannot account for cellular adjustments in chla:$C_{phyto}$ ratios that are not driven by biomass.

Our result shows that more research is needed in order to understand the chl-*a*:$C_{phyto}$ relationship of the Southern Ocean and what drives its variability. This is because of the result we obtained in (Fig.5.5), where increase in depth resulted in increase in chl-*a*:$C_{phyto}$ relationship and little evident of increasing chl-a:$C_{phyto}$ with MLD. It should be noted that it is important to get a good chl-*a*:$C_{phyto}$ if we are to improve current biogeochemical models and our understanding of the role of phytoplankton in the global carbon cycle (Sathyendranath *et al.,* 2009).

This study enabled us to visualize and analyse each method independently. The analysis also suggested that each oceanic region has factors that drive their variability and care needs to be taken when applying a method that was derived from one oceanic region to another. It is therefore essential that additional effort is put into developing methods of estimating $C_{phyto}$ that are region specific.

## Appendix 1

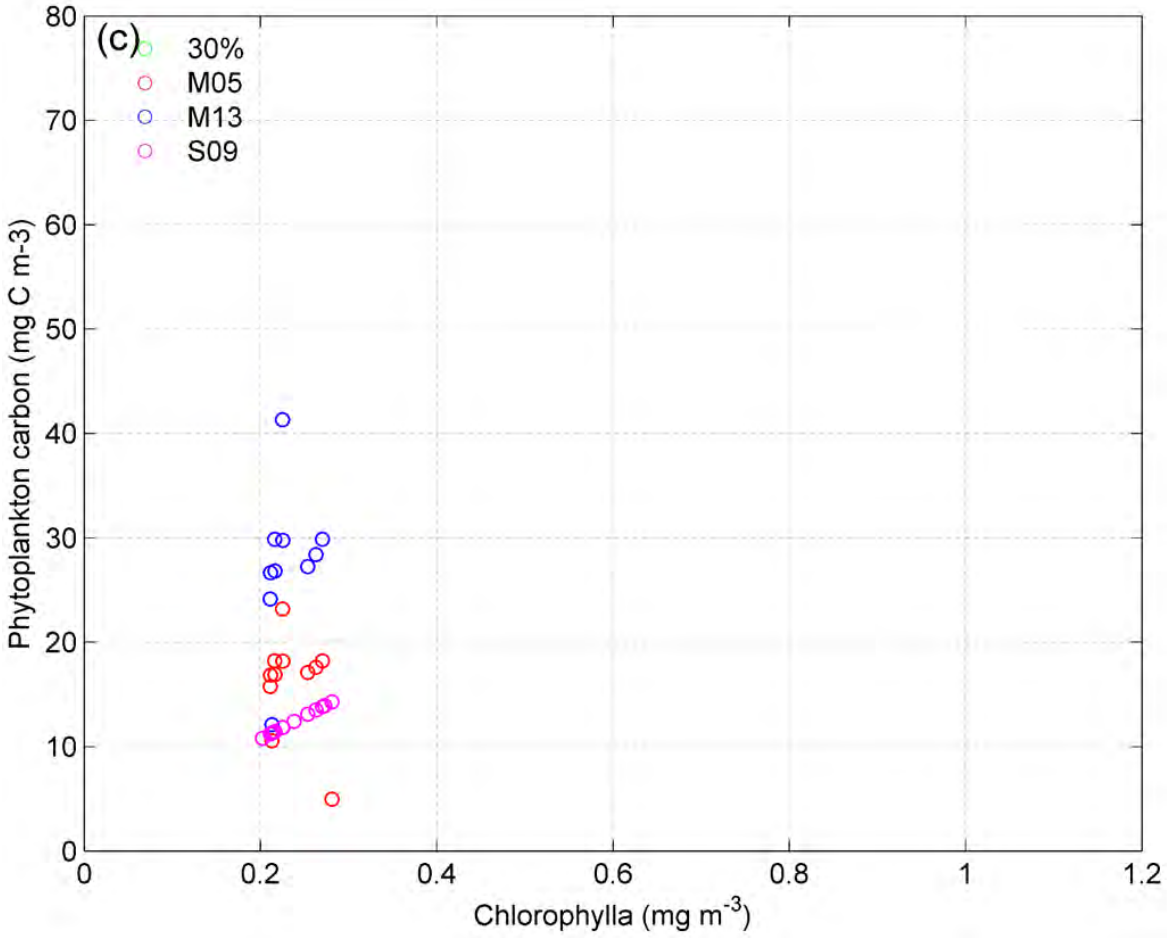


**Figure.** Variation of surface phytoplankton carbon ($C_{phyto}$) and chlorophyll with depth at 120 m. The chlorophyll match the $C_{phyto}$ at the same depth**.**

## References


Abeysirigunawardena, D. S. and Walker, I.J., 2008. Sea level responses to climatic variability and change in Northern British Columbia. *Atmospheric Ocean*, 46, 277–296.

ACE CRC (2011). Position Analysis: Climate change and the Southern Ocean. Prepared by Nathan Bindoff, Steve Rintoul and Marcus Haward. PA06-110825 ISBN 978-0-9871939-0-2

Antoine, D., J.M., Andre and Morel A., 1996. Oceanic primary production, Estimation at global scale from satellite (coastal zone color scanner) chlorophyll, *Global Biogeochemical Cycles 10*, 57-69.

Armstrong, R.A., 2006. Optimality based modeling of nitrogen allocation and photo acclimation in photosynthesis*, Deep Sea Research II* 53: 513-531, ISSN 0967-0645, http://dx.doi.org/10.1016/j.dsr2.2006.01.020.

Atkinson A., 1996. SubAntarctic copepods in an oceanic, low chlorophyll environment: ciliate predation, food selectivity and impact on prey populations. *Marine Ecology Progress Series*. 130: 85-96.

Atkinson, A., Siegel, V., Pakhomov, E. and Rothery, P., 2004. Long-term decline in krill stock and increase in salps within the Southern Ocean. *Nature*, 432: 100-103.

Behrenfeld, M. J., Boss, E., Siegel, D.A. and Shea, D.M., 2005. Carbon-based ocean productivity and phytoplankton physiology from space. *Global Biogeochemical Cycles*, Vol. 19, GB1006, doi: 10.1029/2004GB002299

Behrenfeld, M. J., Randerson, J. T., McClain, C. R., Feldman, G. C., Sietse, O. L., Tucker, C. J., 2001. Biospheric primary production during an ENSO transition. *Science*, 291, 2594– 2597.

Behrenfeld, M.J. and Boss, E., 2003. The beam attenuation to chlorophyll ratio: an optical index of phytoplankton physiology in the surface. *Ocean Deep Sea Research Part Oceanography Research Paper* 50 (12), 1537–1549.

Behrenfeld, M.J. and Milligan A.J., 2013. Photo physiological Expressions of Iron Stress in Phytoplankton. *Annual Review of Marine Science*, 5:217-246.

Bindoff, N., J. Willebrand, V. Artale, A. Cazenave, J. Gregory, S. Gulev, K. Hanawa, C.L. Quéré, S. Levitus, Y. Nojiri, C.K. Shum, L. Talley and Unnikrishnan A., 2007. Observations: oceanic climate change and sea level. Climate Change 2007: The Physical Science Basis. Working Group I Contribution to the Intergovernmental Panel on Climate Change Fourth Assessment Report, S. Solomon, D. Qin, M. Manning, Z. Chen, M. Marquis, K. B. Averyt, M. Tignor and H. L. Miller, Eds., Cambridge University Press, 385-432.

Bishop James K.B., 2009. Autonomous Observation of Ocean Biological Carbon Pump. http://escholarship.org/uc/item/1q5530cp

Boss E. and Pegau, W.S., 2001. "Relationship of light scattering at an angle in the backward direction to the backscattering coefficient". *Applied Optics*. 40, 5503–5507.

Boyce, D. G., Lewis, M. L. and Worm, B., 2010. Global phytoplankton decline over the past century. *Nature,* 466, 591–596.

Briggs M. S., Valerie C., Wilson-Hodge, C., R. D. Preece, Gerald J. Fishman, R. Marc Kippen, P.N. Bhat, William S. Paciesas, Vandiver L. Chaplin, Meegan, C.A., Von Kienlin, Greiner, J., Dwyer, J.R. and Smith, D.M., 2011. Electron-positron beams from terrestrial lightning observed with Fermi GBM.2010GL046259. *Geophysical Research Letters,* Vol. 38, L02808, doi: 10.1029/2010GL046259.

Broecker W. S. and Peng, T.H., 1992. Ocean circulation and climate: Observation and Modelling the Global Ocean. *Nature* 356, 587.

Church, J. A., White,N.E., Konikow, L.F., Domingues, C.M., Cogley J.G., Rignout E., Gregory, J.M., Van den Broeke, M.R., Monaghan, A.J. and Velicogna I., 2011. Revisiting the Earth's sea-level and energy budgets from 1961 to 2008. *Geophysical Research Letters* 38, L18601.

Cloern, J. E., 1996. Phytoplankton bloom dynamics in coastal ecosystems: a review with some general lessons from sustained investigation of San Francisco Bay, California. *Review of Geophysics* 34, 127–168. (doi: 10.1029/96RG00986).

Comiso, J. C., McClain, C. R., Sullivan, C. W., Ryan, J. P. and Leonard, C. L., 1993. Coastal Zone Color Scanner Pigment Concentrations in the Southern Ocean and Relationships to Geophysical Surface Features, *Journal of Geophysical Research* 98, 2419–2451, doi: 10.1029/92jCO2505.

Dall'Olmo G., T. K. Westberry, M. J. Behrenfeld, E. Boss, and Slade, W.H., 2009. Significant contribution of large particles to optical backscattering in the open ocean. *Biogeosciences*, 6, 947–967.

De Boyer M., C.G. Madec, A. S. Fischer, A. Lazar, and Iudicone D., 2004. Mixed layer depth over the global ocean: An examination of profile data and a profile-based climatology, *Journal of Geophysical Research.,* 109, C12003, doi: 10.1029/2004JC002378C12003.

Ducklow, H. W., Baker, K., Martinson, D.G., Quetin, L.B., Ross, R.M., Smith, R.C., Stammerjohn, S.E., Vernet, M. and Fraser, W., 2007. Marine pelagic ecosystems: The Western Antarctic Peninsula. *Philosophical Transaction of the Royal Society B*. 362, 67-94.

DuRand, M. D., Olson R.J. and Chisholm S.W., 2001. Phytoplankton population dynamics at the Bermuda Atlantic Time-series station in the Sargasso Sea*, Deep Sea Research Part II*, 48, 1983–2003.

Encyclopedia Britannica 2014.
http://global.britannica.com/EBchecked/topic/27026/Southern-Ocean.

Eppley R.W, Chavez F.P and Barber R. T., 1992. Standing stocks of particulate carbon and nitrogen in the equatorial Pacific at $150^0$W, *Journal of Geophysical Research 97,655*-661.

Falkowski, P. G., R. Barber and Smetacek, V., 1998. Biogeochemical controls and feedbacks on ocean primary production. *Science 281*, 200-206.

Field, C. B., Behrenfeld, M. J., Randerson, J. T. and Falkowski, P. G., 1998. Primary production of the biosphere: Integrating terrestrial and oceanic components. *Science*, 281, 237–240.

Field, C. B., M. J. Behrenfeld, J. T. Randerson and Falkowski, P.G., 1998. Primary production of the biosphere: Integrating terrestrial and oceanic components, *Science 281*, 237-240.

Gardner, W. D., I. D. Walsh, and Richardson, M.J., 1993. Biophysical forcing on particle production and distribution during a spring bloom in the North Atlantic, *Deep Sea Research Part II,* 40, 171– 195.

Garibotti I. A., Vernet, M., Ferrario, M.E., Smith, R.C., Ross, R.M and Quetin, L.B., 2003. Phytoplankton spatial distribution patterns along the western Antarctic Peninsula (Southern Ocean*). Marine Ecological Progress Series* Vol. 261: 21–39.

Geider R J, MacIntyre H L. and Kana, T M., 1997. Dynamic model of phytoplankton growth and acclimation: responses of the balanced growth rate and the chlorophyll a: carbon ratio to light, nutrient-limitation and temperature*. Marine Ecological Progress Ser*ies 148: 187-200.

Geider, R.J., MacIntyre, H.L. and Kana, T.M., 1998. A dynamic regulatory model of phytoplanktonic acclimation to light, nutrients and temperature. *Limnology and Oceanography* 43 (4), 679–694.

Gregg W.W., Conkright, M.E., Ginoux, P., O'Reilly, J.E and Casey, N.W., 2003. Ocean primary production and climate: Global decadal changes. *Geophysical Research Letters,* Vol. 30, NO. 15, 1809, doi: 10.1029/2003GL016889.

Gruber, N., Gloor, M., Mikaloff Fletcher, S. E., Doney, S. C., Dutkiewicz, S., Follows, M., Gerber M., Jacobson, A.R., Joos, F., Lindsay, K., Menemenlis, D., Mouchet, A., Mueller, S. A. , Sarmiento, J. L. and Takahashi, T., 2009. Oceanic sources, sinks, and transport of atmospheric CO2 *Global Biogeochemical Cycles, 23*, GB1005, doi: 10.1029/2008GB003349.

Gundersen, K., K. M. Orcutt, D. A. Purdie, A. F. Michaels, and Knap, A.H., 2001. Particulate organic carbon mass distribution at the Bermuda Atlantic time-series Study (BATS) site, *Deep Sea Research Part II*, 48, 1697–1718.

Hiscock, M.R., Lance, V.P., Apprill, A.M., Bidigare, R.R., Johnson, Z.I., Mitchell, B.G., Smith Jr, W.O. and Barber, R.T., 2007. Photosynthetic maximum quantum yield increases are an essential component of the Southern Ocean phytoplankton response to iron. Proceedings of the national Academy of Science 105:12 4775-4780.

Honjo, S., R. Franqois S. Manganini, J. Dymond and Collier, R., 2000. Particle fluxes of the interior of the Southern Ocean of the Western pacific sector along $170^0$W. *Deep Sea Research Part II,* 47, 3521-3548

http://www.globalcarbonproject.org/carbonbudget/14/hl-full.htmal Carbon Project 2014.

Jager C.G., Diehl, S. and Schmidt, G.M., 2008. Influence of water-column depth and mixing on phytoplankton biomass, community composition, and nutrients. *Limnology Oceanography* 53(6), 2008, 2361–2373.

Jenouvrier, S., Weimerskirch, H. and Barbraud, C., 2005. Evidence of a shift in the cyclicity of Antarctic seabird dynamics linked to climate. *Proceedings of the Royal Society. B – Biological Sciences* 272, 887-895.

Johnson R., Peter G. Strutton, Simon W. Wright, Andrew McMinn and Meiners, K.M., 2013. Three improved satellite chlorophyll algorithms for the Southern Ocean. *Journal of Geophysical Research*: oceans, volume 118, 3694–3703, doi:10.1002/jgrc.20270.

Knap, A.H., Michaels, A.F. and Close A., 1994. The JGOFS Protocols Intergovernmental Oceanographic Commission, 198pp.

Leblanc K. J., Armand, A.L., P. Assmy, B. Beker, A. Bode, E. Breton, V. Cornet, J. Gibson, M.P. Gosselin, E. Kopczynska, H. Marshall, J. Peloquin, S. Piontkovski, A. J. Poulton, B. Qu´eguiner, R. Schiebel, R. Shipe, J. Stefels, M. A. van Leeuwe, M. Varela, C. Widdicombe, and Yallop, M., 2012. A global diatom database abundance, biovolume and biomass in the world ocean. *Earth System Science Data*, 4, 149–165, www.earth-syst-sci-data.net/4/149/2012/ doi: 10.5194/essd-4-149-2012

Legendre L. and Michaud J., 1999. Chlorophyll *a* to estimate the particulate organic carbon available as food to large zooplankton in the euphotic zone of oceans. *Journal of Plankton Res*earch 21: 2 067-2 083.

Lenton A, B. Tilbrook R. M. Law, D. Bakker, S. C. Doney, N. Gruber, M. Ishii, M. Hoppema, N. S. Lovenduski, R. J. Matear, B. I. McNeil, N. Metzl, S. E. Mikaloff Fletcher, P. M. S. Monteiro, C. Rödenbeck, C. Sweeney, and Takahashi, T., 2013. Sea–air $CO_2$ fluxes in the Southern Ocean for the period 1990–2009. *Biogeosciences*, 10, 4037-4054.

Levitus, S., Antonov, J.I., Boyer, T.P., Baranova,O.K., Garcia, H.E., Locarini, R.A., Mishonov,A.V., regan,J.R., Seidov, D., Yarosh, E.S. and Zweng, M.M., 2012. World ocean heat content and Thermosteric Sea level change (0–2000m) 1955–2010. *Geophysical Research Letter* 39, L10603.

Loisel H. and Morel, A., 1998 Laboratory experiments with phytoplankton cultures showed similar correlations. *Limnology Oceanography* 43, 847.

LÜ S., WANG X. and HAN B., 2009. A field study on the conversion ratio of phytoplankton biomass carbon to chlorophyll-*a* in Jiaozhou Bay, China. Chinese *Journal of Oceanology and Limnology* Vol. 27 No. 4, P. 793-805, 2009 DOI: 10.1007/s00343-009-9221-0.

Marchant H. J. and Murphy E.J., 1994. Interactions at the base of the Antarctic food web. In: El-Sayed SZ (ed) Southern Ocean ecology: the BIOMASS perspective. Cambridge University Press, New York, p 267–285.

Marra, J C. Langdon and Knudson, C.A., 1995. Primary production, water column changes, and the demise of a Phaeocystis bloom at the marine Light –Mixed layers site ($59^0$N, $21^0$W) in the northeast Atlantic Ocean. *Journal of Geophysical Res*earch 100, 6633.

Martinez-Vicente, V., G. Dall'Olmo, G.Tarran, E.Boss and Sathyendranath, S., 2013. Optical backscattering is correlated with phytoplankton carbon across the Atlantic Ocean, *Geophysical Research Letters*,Vol.40,1-5,doi:10.1002/grl.50252,2013.

McNeil, B.I., Tilbrook, B. and Matear, R.J., 2001. Accumulation and uptake of anthropogenic $CO_2$ in the Southern Ocean, South of Australia between 1968and1996. *Journal of Geophysical Research: Ocean* 106,31431–31445.doi:10.1029/ 2000JC000331.

Metzl, N., Tilbrook, B., and Poisson, A., 1999. The annual $fCO_2$ cycle and the air–sea $CO_2$ flux in the Sub-Antarctic Ocean. *Deep Sea Research Part II*, 49,

Monteiro, P. M. S., Schuster, U., Hood, M., Lenton, A., Metzl, N., Olsen, A., Rogers, K., Sabine, C., Takahashi, T., Tilbrook, B., Yoder, J., Wanninkhof, R., Watson, A., 2009. A global sea surface carbon observing system: Assessment of changing sea surface CO2 and air-sea CO2 fluxes, In: Proceedings of the "OceanObs'09: Sustained Ocean Observations and Information for Society" Conference, Venice, Italy, 21-25 September 2009, ESA Publication WPP-306, 2010.

Moore, J. K. and Abbott, M. R., 2000. Phytoplankton chlorophyll distributions and primary production in the Southern Ocean, *Journal of Geophysical Research* 105, 28709–28722, doi: 10.1029/1999jc000043.

Moore, J.K., M.R. Abbott, J.G. Richman, and D.M. Nelson., 2000. The Southern Ocean at the Last Glacial Maximum: A strong sink for atmospheric carbon dioxide. *Global Biogeochemical Cycles*. 14, 455-476.

Niewiadomska K., Claustre, H., Prieur, L and d'Ortenzio, F., 2009. Submesoscale physical-biogeochemical coupling across the Ligurian Current (northwestern Mediterranean) using a bio-optical glider. *Limnology Oceanography* 53(5, part 2), 2008, 2210–2225.

Orsi, A.H., Whitworth III, T and Nowlin Jr, W.D., 1995. On the meridonal extent and fronts of the Antarctic Circumpolar Current. *Deep-Sea research I*, Volume42, Number 5, page 641-673.

Oubelkheir, K., 2001. Biogeochemical characterization of various oceanic provinces through optical indicators over various space and time scales, Ph.D. thesis, 216 pp., Univ. de la Me´diter./CNRS, Marseille, France.

Parsons, T.R., Maita, Y., and Lalli, C.M., 1984. A manual of chemical and biological methods for seawater analysis, Pergamon Press, Oxford, 173 pp.

Rhein, M., S.R. Rintoul, S. Aoki, E. Campos, D. Chambers, R.A. Feely, S. Gulev, G.C. Johnson, S.A.Josey, A. Kostianoy, C. Mauritzen, D. Roemmich, L.D. Talley and Wang, F., 2013. Observations: Ocean. In: Climate Change 2013: The Physical Science Basis. Contribution of Working Group I to the Fifth Assessment Report of the Intergovernmental Panel on Climate Change [Stocker, T.F., D. Qin, G. K. Plattner, Tignor, M., S.K. Allen, J. Boschung, A. Nauels, Y. Xia, V. Bex and P.M. Midgley (edition.)]. Cambridge University Press, Cambridge, United Kingdom and New York, NY, USA.

Richardson, A. D., Black, T.A., Ciais, P., Delbart, N., Friedl, M.A., Gobron, N., Hollinger, D.Y., Kutsch, W.L., Longdoz, B., Luyssaert, S., Migliavacca,M., Leonardo Montagnani, J. William Munger, Moors, E., Piao, S., Rebmann, C., Reichstein, M., Saigusa, N., Tomelleri, E., Vargas, R. and Varlagi, A., 2010. Influence of spring and autumn phenological transitions on forest ecosystem productivity. *Philosophical Transactions of the Royal Society B* 365, 3227–3246. (doi:10.1098/rstb.2010.0102).

Rintoul, S. R., 2011. The Southern Ocean in the Earth System. In: Science Diplomacy: Antarctica, Science and the Govemance of lntemational Spaces.Berkman, P. A. Lang, M.A., Walton, D.W.H., and Young O.R.(Eds.]. Smithsonian Institution Scholarly Press, Washington.

Rintoul, S.R., K. Speer, M. Sparrow, M. Meredith, E. Hofmann, E. Fahrbach C. Summerhayes, A. Worby, M. England, R. Bellerby, S. Speich, D. Costa, J. Hall, M. Hindell, G. Hosie, K. Stansfield, Y. Fukamachi, T. de Bruin, A. Naveira Garabato, K. Alverson, V. Ryabinin, H. C. Shin and Gladyshev, S., 2009. Southern Ocean Observing System (SOOS): rationale and strategy for sustained observations of the southern ocean

Sackman, B.S., Perry, M.J. and Eriksen, C.C., 2008. Seaglider observations of variability in daytime fluorescence quenching of chlorophyll-*a* in Northeastern Pacific coastal waters. *Bio geosciences* 5, 2839–2865.

Sarmiento, J.L., Dunne, J. and Armstrong, R.A., 2004b. Do we now understand the oceans biological pump? U.S. JGOFS News 12, 1-5.

Sathyendranath, S., Venetia Stuart, Anitha Nair, Kenji Oka, Toru Nakane, Heather Bouman, Marie- Hélène Forget, Heidi Maass and Trevor Platt, T., 2009. Carbon-to-chlorophyll ratio and growth rate of phytoplankton in the sea, *Marine Ecological Progress Series* Vol.383:b73-84,

Schlitzer, R., 2002. Carbon export fluxes in the Southern Ocean: Results from inverse modeling and comparisons with satellite based estimates, *Deep Sea Research PartII*,49,1623–1644,doi:10.1016/S0967-0645(02)00004-8.doi: 10.3354/meps07998.

Schmitt, R. W., 2008. Salinity and the global water cycle. *Oceanography*, 21, 12–19. seawater analysis, Pergamon Press, Oxford, 173 pp

Siegenthaler, U. and Sarmiento, J.L., 1993. Atmospheric carbon dioxide and the ocean, *Nature* 365, 119-125.

Smayda, T. J., 1997. What is a bloom? A commentary. *Limnology Oceanography* 42, 1132–1136. (doi: 10.4319/lo.1997.42. 5 part2 1132).

Smetacek, V., 1985. The annual cycle of Kiel Bight plankton. A long-term analysis. Estuaries 8, 145–157. (doi: 10.2307/1351864)

Smith C., Waldron,H., Sandy Thomalla, S. and Lucas, M., 2014. A Bio-Optical Approach to Phytoplankton Community Structure, Physiology and Primary Production in the Southern Ocean. Submitted Maters Thesis to the University of Cape Town.

Smith W.O Jr, and Sakshaug E., 1990. Polar phytoplankton. In: Smith WO Jr (edition) Polar oceanography. Part B. Chemistry, biology, and geology. Academic Press, London, p 477–525

Socal, G., Boldrin, A., Bianchi F., Civitarese, G., Lazzari, A., Rabitti De S., Totti C and Turchetto,M (1999). Nutrient, particulate matter and phytoplankton variability in the photic layer of the Otranto strait. *Journal of Marine System* 20: 381-398.

Sommer, U., Gliwicz, Z. M., Lampert, W. and Duncan, A., 1986. The PEG-model of seasonal succession of planktonic events in fresh waters. *Archive of Hydrobiology* 106, 433–471.

Stramski and Morel, A., 1990. Optical properties of photosynthetic picoplankton in different physiological states as affected by growth irradiance. *Deep Sea Research* 37, pages 245-266.

Stramski D, and Reynolds, R.A., 1993. Diel variation in the optical properties of a marine diatom. *Limnology and Oceanography.* 38, 1347.

Stramski, D., Reynolds, R.A., Kahru, B. M and Mitchell, G., 1999. Estimation of Particulate Organic Carbon in the Ocean from Satellite Remote Sensing. *Science*: Vol. 285 no. 5425 pp. 239-242 DOI: 10.1126/science.285.5425.239

Swart, S., Thomalla, S.J. and Monteiro, P.M.S., 2014. The Seasonal cycle of mixed layer dynamics and phytoplankton biomass in the Sub-Antarctic Zone: A high resolution glider experiment. *Journal of Marine System*. http://dx.doi.org/10.1016/j.jmarsys2014.06.002.

Takahashi, T., Sutherland S, Wanninkhof, R., Sweeney, C., Feely, R.A., Chipman, D.W., Hales, B., Friederich G., Chavez, F., Sabine, C., Watson, A., .Bakker, C.E.B., Schuster, U., Metzl,N., Yoshikawa-Inoue, H., Masao I. K., Midorikawa, T., Nojiri, Y., Kortzingerm, A., Steinhoff, T., Hoppema, M., Olafsson, J., Arnarson, T.S., Tilbrook, B., Johannessen,T., Olsen, A., Bellerby , R., Wong, C.S., Delille, B., Bates, N.R. and de Baar, J.W., 2009. Climatological mean and decadal change in surface ocean pCO2, and net sea-air flux over the global oceans. *Deep Sea Research II* 56:554-577

Talley, L., Chereskin, T., Dickson,A.,Fine, R., Farias, L., Ulloa, O. and Sloyan, B., 2008. AIW formation in the southeast Pacific. *http://www.pord.ucsd.edu/~ltalley/aaiw/Updated* October 23 2008.

Taylor A H, Geider R J. and Gilbert F. J. H., 1997. Seasonal and latitudinal dependencies of phytoplankton carbon to chlorophyll a ratios: results of a modeling study. *Marine Ecology Programe Series* 152: 51-66.

Thomalla, S., Racault, M., Swart, S., Monteiro, P.M., 2014. High-resolution view of the spring bloom initiation and net community production in the SubAntarctic Southern Ocean using glider data. *Journal of Marine Science*. Submitted.

Trull, T., Bray, S., Manganini, S., Honjo, S., Francois, R., 2001a. Moored sediment trap measurements of carbon export in the Subantarctic and Polar Frontal Zones of the Southern Ocean, south of Australia. *Journal of Geophysical Research Ocean* 106, 31489–31509.doi:10.1029/2000JC000308.

Tynan C. T., 1998. Ecological importance of the Southern Boundary of the Antarctic Circumpolar Current. *Nature* 392, 708-710 doi: 10.1038/33675.

Volk, T. and Hoffert, M.I., 1985. Oceanic carbon pumps: analysis of relative strengths and efficiencies in ocean-driven atmospheric CO2. In: *The Carbon Cycle and Atmospheric $CO_2$: Natural Variations Archean to Present,* edition E. T. Sunquist, W. S. Broecker, page 99-110. Washington, DC, American Geophysical Union, Geophysical Monography, 32.

Von Bröckel K., 1981. The importance of nanoplankton within the pelagic Antarctic ecosystem. *Kiel Meeresforsch Sonderh* 5:61–67.

Wang, X., Matear, R., Trull, T., 2001. Modeling seasonal phosphate export and resupply in the sub Antarctic and Polar Frontal Zones in the Australian sector of the Southern Ocean. *Journal of Geophysical Research Ocean* 106, 315253141 doi: 10.1029/2000JC000645

Watson A J., Meredith M P. and Marshall J.., 2014. The Southern Ocean, carbon and climate. *Philosophical Transaction of the Royal Society* A372:20130057. http://dx.doi.org/10.1098/rsta.2013.0057.

Westberry, T., M. J. Behrenfeld, D. A. Siegel, and Boss, E., 2008. Carbon-based primary productivity modeling with vertically resolved photo acclimation, *Global Biogeochemical Cycles 22*, GB2024, doi: 10.1029/2007GB003078.

Winder M. and Cloern, J.E., 2010. The annual cycles of phytoplankton. *Philosophical Transaction Royal Society B*365, 3215–3226 doi:10.1098/rstb.2010.0125.

Yool, A., Martin, A.P., Fernandez, C. and Clark, R.J., 2007. Not so new the significance of nitrification for oceanic "new" production, *Nature* 447, 999-1002.

Zang Z., Hu,Z., Li, Z., He, Q.and Chang ,X., 2009. Synthesis, characterization and application of ethylenediamine-modified multiwalled carbon nanotubes for selective solid-phase extraction and pre-concentration of metal ions. *Journal of Hazardous Materials* 172 958–963.